


Nonparanormal Modeling Framework for Prognostic Biomarker Assessment with Application to Amyotrophic Lateral Sclerosis

Ainesh Sewak^{}
Universität Bern

Vanda Inácio^{}
University of Edinburgh

Joanne Wu^{}
University of Miami

Michael Benatar^{}
University of Miami

Torsten Hothorn^{}
Universität Zürich

Abstract

Identifying reliable biomarkers for predicting clinical events in longitudinal studies is important for accurate disease prognosis and the development of new treatments. However, prognostic studies are often not randomized, making it difficult to account for patient heterogeneity. In amyotrophic lateral sclerosis (ALS), factors such as age, site of disease onset and genetics impact both survival duration and biomarker levels, yet their impact on the prognostic accuracy of biomarkers over different time horizons remains unclear. While existing methods for time-dependent receiver operating characteristic (ROC) analysis have been adapted for censored time-to-event outcomes, most do not adjust for patient covariates. To address this, we propose the nonparanormal prognostic biomarker (NPB) framework, which models the joint dependence between biomarker and event time distributions while accounting for covariates. This provides covariate-specific ROC curves which assess a potential biomarker's accuracy for a given time horizon. We apply this framework to evaluate serum neurofilament light (NfL) as a biomarker in ALS and demonstrate that its prognostic accuracy varies over time and across patient subgroups. The NPB framework is broadly applicable to other conditions and has the potential to improve clinical trial efficiency by refining patient stratification and reducing sample size requirements.

Keywords: prognostic biomarkers, amyotrophic lateral sclerosis, time-dependent ROC analysis, Gaussian copula, semiparametric transformation model, covariates.

1. Introduction

Prognostic biomarkers are essential tools in predicting clinical events, enabling better patient stratification and setting eligibility criteria for clinical trials. As the identification of new biomarkers grows, it becomes increasingly important to have methods for evaluating their accuracy. Since a biomarker's prognostic accuracy may differ across patient subgroups, evaluating how it varies with covariates is important for determining its clinical utility.

In prognostic biomarker evaluation studies, the key questions are: How accurately can a baseline biomarker predict the future occurrence of a clinical event? How do patient co-

variates influence this accuracy? And how well can the biomarker predict future rates of functional decline? Unlike diagnostic studies, where both the disease outcome and biomarker are measured at baseline, prognostic studies require assessing the baseline biomarker’s ability to predict outcomes over time.

The most common way in medical research is to summarize a biomarker’s prognostic accuracy using a hazard ratio from a proportional hazards model. However, this is an incomplete measure of prognostic accuracy (Bansal and Heagerty 2019). As Pepe *et al.* (2004) demonstrated for odds ratios in diagnostic accuracy, a measure of association such as the hazard ratio does not directly capture how well a biomarker can discriminate patients at higher risk of experiencing the event within a given time-horizon. Moreover, the proportional hazards assumption is often violated, making hazard ratios unreliable if applied by default (Stensrud and Hernàn 2025). Relying solely on this approach risks overlooking important time-varying and covariate-specific differences in prognostic accuracy.

This has led to the development of time-dependent versions of traditional accuracy measures, such as sensitivity, specificity, the receiver operating characteristic (ROC) curve, and the area under the ROC curve (AUC). Various approaches for time-dependent sensitivity and specificity have been proposed (Slate and Turnbull 2000; Heagerty and Zheng 2005; Cai *et al.* 2006). In this paper, we focus on the cumulative sensitivity and dynamic specificity which are the most widely used in clinical applications (Lambert and Chevret 2016). While there is extensive literature on estimating time-dependent ROC curves (see Blanche *et al.* 2013b; Kamarudin *et al.* 2017, for a review and references therein), copula-based approaches for modeling biomarker and event time distributions remain relatively unexplored but offer a flexible way to capture dependence structures (Escarela *et al.* 2023).

Further, only a limited number of methods incorporate covariates in prognostic biomarker evaluation, leaving a gap in addressing patient heterogeneity. Ignoring this heterogeneity can lead to biased estimates of a biomarker’s accuracy (Janes and Pepe 2008). Three main approaches have been proposed to adjust for covariates in the prognostic setting. The first assumes a proportional hazards model for event time given the biomarker and covariates (Song and Zhou 2008; Li and Ning 2015), but this strong assumption can bias accuracy estimates if violated. The second, a fully nonparametric kernel smoothing approach, estimates the joint distribution of the biomarker, event time, and covariates but is limited to a single continuous covariate (Rodríguez-Álvarez *et al.* 2016). The third approach includes more recent methods, such as standardizing the marker distribution via inverse probability weighting (Le Borgne *et al.* 2018), averaging covariate-specific ROC curves over the covariate distribution (Dey *et al.* 2023) and estimating summary indices of covariate-specific time-dependent ROC curves (Jiang *et al.* 2024).

This paper proposes a modeling framework for covariate-specific ROC analysis. The approach employs semiparametric marginal models for the biomarker and event time distributions, linked through a Gaussian copula to capture their joint dependence. Estimation is performed using the nonparanormal likelihood, which accommodates right- and interval-censored data. This framework enables the derivation of model-based covariate-specific time-dependent ROC curves and summary indices.

The layout of the paper is as follows. We begin with a motivating example in Section 2, using biomarker and event time data from a longitudinal study on amyotrophic lateral sclerosis (ALS). Section 3 introduces key concepts, including sensitivity, specificity and the covariate-

specific cumulative-dynamic ROC curve. In Section 4 we present the technical details of our model, including parameterization and inference. Section 5 provides results from a simulation study with a detailed comparison to existing methods. In Section 6 we apply our method to the ALS study data. Finally, we explore potential extensions of our approach in Section 7 and offer concluding remarks in Section 8.

2. Prognostic biomarkers in ALS

ALS is a progressive neurodegenerative disease that causes degeneration of nerve cells, leading to muscle weakness, paralysis and respiratory failure. With a median survival duration of 20 to 48 months after symptom onset, ALS currently has no cure, and available treatments primarily aim to manage the symptoms and slow disease progression (Feldman *et al.* 2022). Identifying reliable prognostic biomarkers for ALS are essential for improving clinical trial design (Kiernan *et al.* 2021; Benatar *et al.* 2024). Biomarkers may be utilized in trial designs to stratify patients into homogeneous subgroups, serve as eligibility criteria to define appropriate study populations, and act as baseline covariates to adjust for patient heterogeneity. Together, these applications reduce sample size requirements, enable more cost-effective studies, and accelerate the development of effective treatments (Taga and Maragakis 2018).

2.1. Longitudinal ALS cohort

The methods developed in this article are motivated by a prospective longitudinal study on the prognostic utility of neurofilament biomarkers for amyotrophic lateral sclerosis (ALS), as described by Benatar *et al.* (2020). One of the outcomes of the study was survival duration, defined as the time from the baseline visit to either permanent assisted ventilation, tracheostomy, or death. Patients who did not experience any of these events during the follow-up period were right-censored. Our study analyzed a subset of 260 patients enrolled across multiple clinical sites through the Clinical Research in ALS and Related Disorders for Therapeutic Development (CRATE) Consortium’s Phenotype-Genotype-Biomarker study (registered at clinicaltrials.gov: NCT02327845), representing the data available for biomarker analysis at the time of a prior publication (Benatar *et al.* 2020). Patients included in the present study comprised 229 patients with ALS, 11 with progressive muscle atrophy (PMA), and 20 with primary lateral sclerosis. To discover and validate biomarkers, all patients underwent systematic follow-ups with standardized clinical evaluations and provided biological samples every 3 to 6 months. For our analysis, we included patients with ALS or PMA. After excluding 12 patients with missing values in one or more covariates, the final sample comprised $N = 218$ patients.

The biomarker of interest in our study is serum neurofilament light (NfL) concentration. Baseline serum NfL concentration has been shown to differentiate ALS patients from healthy controls and is associated with both survival outcomes and disease progression in ALS (Lu *et al.* 2015; Benatar *et al.* 2024). Figure 1 illustrates the observed relationship between baseline NfL and survival duration in the present study, showing that higher baseline NfL levels are generally associated with shorter survival. However, this association is not strictly linear and any evaluation of prognostic accuracy must account for the right-censored data in the study. Furthermore, the prognostic accuracy of NfL may depend on the time horizon of prediction and could be influenced by patient characteristics.

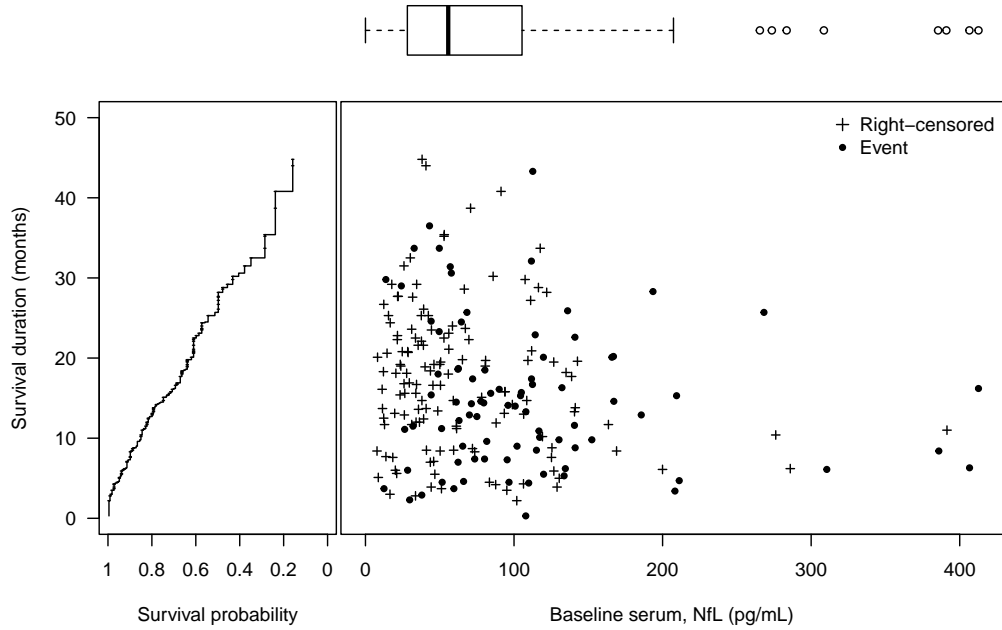


Figure 1: Scatter plot of the observed baseline serum neurofilament light (NfL) concentration (pg/mL) and survival duration (in months since baseline). Right censored subjects are indicated with “+” and subjects who reached the endpoint are marked by “•”.

2.2. Challenges in assessing prognostic accuracy

Evaluating the prognostic accuracy of ALS biomarkers in observational studies is challenging because of the risk of confounding. Confounding arises when covariates such as age are associated with both biomarker levels and disease prognosis. For example, older patients tend to have elevated NfL levels and face an increased risk of ALS-related mortality, potentially distorting the accuracy of NfL as a prognostic marker. While factors such as aging and site of onset are known to be associated with NfL levels, their impact on NfL’s prognostic accuracy across different time horizons remains unclear (Koini *et al.* 2021; Benatar *et al.* 2023).

Stratifying by covariates can help address confounding, but this approach is limited to a small number of categorical covariates and often results in small sample sizes in each group, limiting the ability to draw statistically efficient conclusions. In ALS, where large datasets are scarce, proportional hazards models are commonly used to estimate an overall hazard ratio. Such regression models account for confounding and can give an indication of the prognostic utility of NfL by quantifying its association with survival duration. However, they do not fully capture how NfL’s prognostic accuracy changes across different time horizons. Additionally, these models assume that the relationship between NfL, covariates, and survival duration remains proportional over time. This is a condition that may not hold in a progressive disease like ALS, where risk dynamics evolve (Stensrud and Hernàn 2025).

To address these limitations, covariate-specific sensitivity and specificity can be used to assess a biomarker’s ability to predict survival. These measures form the foundation of ROC analysis and provide a framework for evaluating prognostic accuracy across different time horizons.

3. Evaluation of prognostic biomarkers

We first provide a brief overview of evaluating the accuracy of a continuous biomarker Y in predicting a time-constant binary outcome D , where $D = 0$ represents “controls” and $D = 1$ represents “cases”. Assuming higher values of Y are more indicative of disease, a threshold $c \in \mathbb{R}$ can be used to classify subjects as cases if their biomarker value exceeds c , and as controls otherwise. Sensitivity is the correct classification probability for cases, defined as $\text{Se}(c) = \text{P}(Y > c \mid D = 1)$, while specificity represents the correct classification probability for controls, $\text{Sp}(c) = \text{P}(Y < c \mid D = 0)$. For any given biomarker, there is a trade-off between sensitivity and specificity, as increasing one decreases the other. This trade-off is determined by the choice of c . The ROC curve is a graphical tool that plots sensitivity against $1 - \text{specificity}$ for all possible threshold values of c and provides a measure of the biomarker’s diagnostic accuracy.

Most diseases do not present binary outcomes. Instead, they often involve longitudinal outcomes, such as survival duration for ALS patients. To accommodate this, various extensions have been developed to measure time-dependent sensitivity and specificity (Heagerty and Zheng 2005). We focus on the cumulative sensitivity and dynamic specificity because our interest lies in evaluating the accuracy of prognostic ALS biomarkers at specific time points. Specifically, we would like to estimate the accuracy of the biomarker in predicting outcomes such as one-year survival. Additionally, both the biomarker and survival duration might depend on a set of covariates $\mathbf{X} = (X_1, \dots, X_p)$ such as age, sex, genetic factors and disease progression which need to be taken into account.

For the event time T , we define the covariate-specific cumulative sensitivity and dynamic specificity as

$$\begin{aligned} \text{Se}_t^{\text{C}}(c \mid \mathbf{x}) &= \text{P}(Y > c \mid T \leq t, \mathbf{X} = \mathbf{x}) \\ \text{Sp}_t^{\text{D}}(c \mid \mathbf{x}) &= \text{P}(Y \leq c \mid T > t, \mathbf{X} = \mathbf{x}). \end{aligned}$$

In this context, *cumulative* sensitivity considers any subject who experiences the event before a time point of interest t as a case (i.e., $T \leq t$, or conceptually, $D(t) = 1$), while *dynamic* specificity defines a control as any subject who remains event-free at time t (i.e., $T > t$, or $D(t) = 0$). For a fixed time t , the entire population is thus classified into cases (those who have experienced the event) and controls (those still at risk).

These definitions lead to the *cumulative-dynamic* ROC curve, which assesses the biomarker’s prognostic accuracy for a given time horizon. This enables evaluation of how effectively a baseline marker can differentiate between subjects who will experience the event of interest and those who will not within a specified follow-up interval. Each time horizon of interest may yield a different accuracy, reflecting the dynamic nature of time-to-event data. The covariate-specific cumulative-dynamic ROC curve is given by

$$\text{ROC}_t^{\text{C/D}}(p \mid \mathbf{x}) = \text{Se}_t^{\text{C}} \left([1 - \text{Sp}_t^{\text{D}}]^{-1}(p \mid \mathbf{x}) \mid \mathbf{x} \right), \text{ for } p \in [0, 1],$$

where the function $[1 - \text{Sp}_t^{\text{D}}]^{-1}(p) = \inf \{y \in \mathbb{R} : 1 - \text{Sp}_t^{\text{D}}(y) \leq p\}$ exists. These definitions allow for assessing a biomarker’s prognostic accuracy for subjects with shared characteristics $\mathbf{X} = \mathbf{x}$.

The area under the cumulative-dynamic ROC curve (AUC) is the most widely used summary measure of the ROC curve and represents the probability that a subject with a higher

biomarker value experienced the event earlier. The corresponding covariate-specific time-dependent AUC is defined as

$$\text{AUC}_t(\mathbf{x}) = \int_0^1 \text{ROC}_t^{\text{C/D}}(p | \mathbf{x}) dp = \text{P}(Y_i > Y_j | T_j < T_i, \mathbf{X} = \mathbf{x})$$

for two distinct subjects i and j . Other measures, such as the Youden Index and optimal cut-off values, can also be derived once the ROC curve is obtained. Although this paper focuses on the cumulative-dynamic ROC curve, the methods discussed can estimate other forms of time-dependent ROC curves in the same statistical framework as well. Additional details for these approaches are provided in Supplementary Material A.

4. The nonparanormal prognostic biomarker model

The Nonparanormal Prognostic Biomarker (NPB) model consists of two main components: (1) a joint model capturing the dependence between the biomarker and event time, and (2) marginal models for each incorporating the effects of covariates.

Using Bayes' theorem, for a fixed time t , the cumulative sensitivity can be expressed as

$$\text{Se}_t^{\text{C}}(c | \mathbf{x}) = \frac{\text{P}(Y > c, T \leq t | \mathbf{X} = \mathbf{x})}{\text{P}(T \leq t | \mathbf{X} = \mathbf{x})} = \frac{F_T(t | \mathbf{x}) - F_{Y,T}(c, t | \mathbf{x})}{F_T(t | \mathbf{x})},$$

where $F_T(t | \mathbf{x})$ is the marginal distribution of the event time conditioned on the covariates \mathbf{x} and $F_{Y,T}(y, t | \mathbf{x})$ is the joint conditional CDF of the biomarker and event time. Similarly, the dynamic specificity at time t is given by

$$\text{Sp}_t^{\text{D}}(c | \mathbf{x}) = \frac{\text{P}(Y \leq c, T > t | \mathbf{X} = \mathbf{x})}{\text{P}(T > t | \mathbf{X} = \mathbf{x})} = \frac{F_Y(c | \mathbf{x}) - F_{Y,T}(c, t | \mathbf{x})}{1 - F_T(t | \mathbf{x})},$$

where $F_Y(c | \mathbf{x})$ is the marginal distribution of the biomarker. Notice that if the joint conditional distribution of (Y, T) given $\mathbf{X} = \mathbf{x}$ is known, all terms in these expressions can be derived. Further, we can calculate cumulative sensitivity and dynamic specificity for a range of cut-off points $c \in \mathbb{R}$ and plot the corresponding ROC curve for a specific time t conditional on covariate values \mathbf{x} . The time-dependent covariate-specific AUC can then be obtained by numerically integrating the corresponding ROC curve.

Previous methods have faced challenges in incorporating censoring, often leading to approaches that either rely on proportional hazards models for event time or use nonparametric Kaplan-Meier estimators, which cannot account for covariate dependence. In this paper, we focus on flexibly modeling the joint conditional distribution $F_{Y,T}(y, t | \mathbf{x})$ of the biomarker and event time given $\mathbf{X} = \mathbf{x}$. This approach allows us to calculate model-based covariate-specific cumulative sensitivity, dynamic specificity, and construct time-dependent covariate-specific ROC curves and corresponding summary metrics such as $\text{AUC}_t(\mathbf{x})$. Next, we detail the components of the model followed by a likelihood-based estimation approach that can accommodate both right and interval censoring schemes.

4.1. Joint model specification

Semiparametric regression models that account for covariate effects are well-established for modeling either the biomarker distribution (Pepe 1997) or the event time distribution (Cox

1972), both of which may be subject to censoring. However, modeling the joint conditional distribution of the biomarker and event time poses additional challenges, particularly when incorporating the dependence between these two variables. To address this, we use the non-paranormal model (Liu *et al.* 2009), which allows us to combine the marginal distributions of Y and T through a Gaussian copula function with correlation parameter $\rho \in [-1, 1]$ and model the joint conditional distribution as

$$\begin{aligned} F_{Y,T}(y, t | \mathbf{x}) &= \mathbf{P}(Y \leq y, T \leq t | \mathbf{X} = \mathbf{x}) \\ &= C_\rho(F_Y(y | \mathbf{x}), F_T(t | \mathbf{x})) \\ &= \Phi_\rho(\Phi^{-1}(F_Y(y | \mathbf{x})), \Phi^{-1}(F_T(t | \mathbf{x}))) \end{aligned}$$

where Φ denotes the CDF of a standard normal distribution and $\Phi_\rho(z_1, z_2)$ is the CDF of the bivariate standard normal distribution with correlation ρ and corresponding density $\phi_\rho(z_1, z_2)$. The copula captures the dependence structure between the biomarker and event time, separating it from their marginal distributions. We define monotonically nondecreasing marginal transformation functions as

$$h_Y(y | \mathbf{x}) = \Phi^{-1}(F_Y(y | \mathbf{x})) \text{ and } h_T(t | \mathbf{x}) = \Phi^{-1}(F_T(t | \mathbf{x})),$$

which map the unknown conditional distribution of $(Y, T) | \mathbf{X} = \mathbf{x}$, to a known latent bivariate standard normal distribution $\mathbf{Z} = (h_Y(Y | \mathbf{x}), h_T(T | \mathbf{x}))^\top \sim N_2\left(\mathbf{0}, \begin{pmatrix} 1 & \rho \\ \rho & 1 \end{pmatrix}\right)$. Although each marginal distribution could involve a different set of covariates, for notational simplicity, we assume the same set of covariates throughout.

4.2. Marginal model parameterization

We model the marginal distributions semiparametrically using probit linear transformation models

$$F_Y(y | \mathbf{x}) = \Phi\left(h_Y(y) - \mathbf{x}^\top \boldsymbol{\beta}_Y\right) \text{ and } F_T(t | \mathbf{x}) = \Phi\left(h_T(t) - \mathbf{x}^\top \boldsymbol{\beta}_T\right),$$

where h_Y and h_T are baseline transformation functions that map the biomarker Y and event time T to the latent normal scale, and $\boldsymbol{\beta}_Y$ and $\boldsymbol{\beta}_T$ are the respective linear covariate effects. Under this specification, the joint conditional CDF is given by

$$F_{Y,T}(y, t | \mathbf{x}) = \Phi_\rho\left(h_Y(y) - \mathbf{x}^\top \boldsymbol{\beta}_Y, h_T(t) - \mathbf{x}^\top \boldsymbol{\beta}_T\right), \quad (1)$$

and the joint conditional density function for this model is given by

$$f_{Y,T}(y, t | \mathbf{x}) = \phi_\rho\left(h_Y(y) - \mathbf{x}^\top \boldsymbol{\beta}_Y, h_T(t) - \mathbf{x}^\top \boldsymbol{\beta}_T\right) h'_Y(y) h'_T(t). \quad (2)$$

As in Hothorn *et al.* (2018), we model the baseline transformation function for the biomarker as a monotonically nondecreasing smooth function of y , defined as

$$h_Y(y | \boldsymbol{\vartheta}_Y) = \mathbf{b}(y)^\top \boldsymbol{\vartheta}_Y = \sum_{m=0}^M \vartheta_{Y,m} b_m(y),$$

where $\mathbf{b}(y) = (b_0(y), \dots, b_M(y))^\top$ is a vector of $M + 1$ basis functions with coefficients $\boldsymbol{\vartheta}_Y \in \mathbb{R}^{M+1}$. The parameter M controls the degree of smoothing. We use polynomials in Bernstein form as the basis functions because if the order M is chosen to be sufficiently large, Bernstein polynomials can uniformly approximate any real-valued continuous function on an interval (Farouki 2012). Additionally, the constraints $\vartheta_{Y,m} \leq \vartheta_{Y,m+1}$ for $m = 0, \dots, M - 1$ guarantee the monotonicity of h_Y . The Bernstein basis polynomial of order M on the interval $[l, u]$ is given by

$$b_m(y) = \binom{M}{m} \tilde{y}^m (1 - \tilde{y})^{M-m}, \quad m = 0, \dots, M,$$

where the observations are pre-normalized $\tilde{y} = \frac{y-l}{u-l}$. The baseline transformation function for event time is parameterized analogously and we denote the coefficients of the corresponding basis functions as $\boldsymbol{\vartheta}_T$.

4.3. Likelihood inference

The complete set of parameters for our model is denoted as $\boldsymbol{\theta} = (\boldsymbol{\vartheta}_Y^\top, \boldsymbol{\vartheta}_T^\top, \boldsymbol{\beta}_Y^\top, \boldsymbol{\beta}_T^\top, \rho)^\top$. The likelihood in our model corresponds to the ‘‘mixed nonparanormal likelihood’’ with smooth parameterization of the marginal transformation functions (Hothorn 2024b). This mixed likelihood structure accommodates both censored and continuous responses. It results in a ‘‘flow nonparanormal likelihood’’ for continuous variables and an interval-censored likelihood defined by the conditional distribution of censored time-to-event observations. In the bivariate case relevant here, our model accounts for two primary types of censoring: exact and interval-censored observations. Assume we observe N_e exact and N_c interval censored observations, for a total of $N = N_e + N_c$ observations.

For observations with uncensored (exact) biomarker and event times, we observe $O_i = (y_i, t_i, \mathbf{x}_i)$ for $i = 1, \dots, N_e$. The likelihood contribution in this case is given by the conditional joint density of the model

$$\ell_e(\boldsymbol{\theta} | O_i) = f_{Y,T}(y_i, t_i | \mathbf{x}_i, \boldsymbol{\theta})$$

as defined in Equation 2.

For exact biomarker measurements with interval-censored event times assumed to be conditionally independent, we observe $O_i = (y_i, \underline{t}_i, \bar{t}_i, \mathbf{x}_i)$ for $i = N_e + 1, \dots, N$ where $(\underline{t}_i, \bar{t}_i)$ defines the interval for the censored event time. The likelihood contribution in this case is given by

$$\begin{aligned} \ell_c(\boldsymbol{\theta} | O_i) &= F_{Y,T}(y_i, \bar{t}_i | \mathbf{x}_i) - F_{Y,T}(y_i, \underline{t}_i | \mathbf{x}_i) \\ &= \int_{h_T(\underline{t}_i | \boldsymbol{\vartheta}_T)}^{h_T(\bar{t}_i | \boldsymbol{\vartheta}_T)} \phi_\rho \left(h_Y(y_i | \boldsymbol{\vartheta}_Y) - \mathbf{x}_i^\top \boldsymbol{\beta}_Y, z_T - \mathbf{x}_i^\top \boldsymbol{\beta}_T \right) h'_Y(y_i) dz_T. \end{aligned}$$

Here, ϕ_ρ represents the joint density component, and the integral captures the likelihood contribution across the interval for censored event times. Notice that right-censored event times can be treated as a special case of this likelihood where $\bar{t}_i = \infty$. With these individual likelihood contributions, we construct the joint log-likelihood for the dataset as

$$\ell(\boldsymbol{\theta} | \mathbf{O}) = \sum_{i=1}^{N_e} \log(\ell_e(\boldsymbol{\theta} | O_i)) + \sum_{i=N_e+1}^N \log(\ell_c(\boldsymbol{\theta} | O_i)),$$

where $\mathbf{O} = \{O_1, \dots, O_N\}$ represents the full dataset, including both exact and interval-censored observations. The maximum likelihood estimate of $\boldsymbol{\theta}$ is derived by using constrained maximization algorithms which involves evaluating multivariate normal probabilities. These probabilities are computed using randomized quasi-Monte Carlo integration methods (Genz 1992). The score functions for the parameters have been described in detail by Hothorn (2024b) and are implemented in the `mvtnorm` add-on package (Hothorn 2024a).

4.4. Model assessment

Our modeling approach relies on the dependence between the biomarker and event time distributions being captured by a correlation parameter in the Gaussian copula. Dette *et al.* (2014) demonstrated that a large class of commonly used parametric copula models cannot produce nonmonotone regression functions. This is evident from the following expression for the conditional distribution function of time-to-event given biomarker and covariates

$$P(T \leq t \mid Y = y, \mathbf{X} = \mathbf{x}) = \Phi \left(\frac{h_T(t) - \rho h_Y(y) + \mathbf{x}^\top (\rho \boldsymbol{\beta}_Y - \boldsymbol{\beta}_T)}{1 - \rho^2} \right)$$

obtained from our joint model. Notice that $h_Y(y)$ is monotonically increasing in y . To validate if the assumption that the correlation parameter is sufficient to capture the dependence structure between the biomarker and event time from our model, we can check if the conditional distribution function of T is indeed monotonic with respect to y . This can be achieved by fitting a semiparametric smooth mixed effects additive transformation model which transforms the event time and includes a smooth term for the biomarker as part of the regression (Tamási 2025). If the smooth term is either monotonically increasing or decreasing, the assumption is not violated. However, if the smooth term exhibits nonmonotonic behavior, the Gaussian copula dependence structure may not be appropriate for the data.

5. Empirical evaluation

In this section, we use simulated data to evaluate the performance of our NPB model in assessing the prognostic accuracy of biomarkers. Since most existing methods for time-dependent ROC analysis do not account for covariates, we begin by comparing these methods in the unconditional scenario, followed by a comparison when covariates are introduced. For competitor methods in the unconditional case, we considered actively maintained R packages that are hosted and quality assured on the Comprehensive R Archive Network (CRAN), as summarized in Table 1. For a review of these methods, see Kamarudin *et al.* (2017).

We label each method using the R package name, followed by an abbreviation for the specific estimator when multiple options are available within the same package.

5.1. Data generating process

For the biomarker, we as data generating process (DGP) considered the following distributions F_Y : standard normal $N(0, 1)$, two-component normal mixture of $N(1, 1)$ and $N(4, 1.5^2)$ with equal mixture weights, and the Chi-squared with three degrees of freedom. For event time, we used the following distributions F_T : standard lognormal, Weibull with shape 1.4 and rate 2.0, and Gamma with shape 1.5 and rate 1.2. We explored all combinations of biomarker and

Package	Methods	Reference
survivalROC	Nearest neighbor estimation (NNE), Kaplan-Meier (KM)	Heagerty <i>et al.</i> (2000)
timeROC	Inverse probability weighting (IPW)	Blanche <i>et al.</i> (2013a)
smoothROctime	Bivariate kernel density estimation	Martínez-Cambolor and Pardo-Fernández (2018)
nsROC	Cox proportional hazards model (COX), Kaplan-Meier (KM) and weighted Kaplan-Meier (WKM)	Pérez-Fernández <i>et al.</i> (2018)
cenROC	Weighted kernel smoother with (TR) and without boundary correction (UTR)	Beyene and El Ghouch (2020)
tdROC	Nonparametric weight adjustments	Li <i>et al.</i> (2018)

Table 1: R packages and methods for unconditional time-dependent ROC analysis.

event time distributions, with sample sizes of $N \in \{100, 500, 1000\}$ for a 1000 replications. This data generation approach is similar to that used in previous studies (Martínez-Cambolor and Pardo-Fernández 2018; Yu and Hwang 2019; Beyene and Chen 2024).

We generated $\mathbf{Z} = (Z_1, Z_2)^\top$ from a standard bivariate normal distribution with correlation coefficient $\rho \in \{-0.3, -0.5\}$. The negative correlation implies that higher baseline biomarker concentrations are associated with shorter event times. To explore the range of marginal distributions, we transformed the marginals to uniform distributions $(U_1, U_2) = (\Phi(Z_1), \Phi(Z_2))$ and applied different quantile functions to obtain the desired distributions of the biomarker and event time (Y, T) . This preserves the dependence structure governed by ρ while allowing the marginal distributions to vary.

To achieve an expected censoring rate of 50%, the censoring time C can be generated independently following the same distribution as the event time. For any other censoring rate $\kappa = \mathbb{P}(T > C)$, independent realizations can be drawn from a distribution of the same form as the event time, given by $F_C(c) = \Phi(h_T(c) + a)$, where $a = \Phi^{-1}(\kappa)\sqrt{2}$ is an offset based on the definition of the AUC used to achieve the target censoring rate (Sewak and Hothorn 2023). In our study, we applied censoring rates of $\kappa \in \{0.3, 0.5\}$.

5.2. Unconditional results

We evaluated the AUC at times corresponding to the unconditional quantiles 0.1, 0.25, 0.5, and 0.75 for each estimator and biomarker distribution. Figure 3 displays the mean and standard error across the 1000 repetitions of the estimated AUC for different methods and sample sizes. The NPB method shows a small bias for small sample sizes but is generally unbiased for larger sample sizes across different time quantiles and biomarker distributions. Additionally, the NPB model demonstrates lower variability compared to other methods. In contrast, the NNE estimator from **survivalROC** exhibits bias in all scenarios. Most methods are unbiased for time quantiles below 0.5, but **smoothROctime** and **nsROC** have some bias for higher time quantiles. The results were consistent across different event time distributions. Results for a lognormal event time distribution, a 50% censoring rate and a correlation of

$\rho = -0.7$ are shown in Supplementary Figure 9.

For the ROC curve, we calculated the root integrated squared error (RISE)

$$\text{RISE} = \sqrt{\int_0^1 (\widehat{\text{ROC}}_t(p) - \text{ROC}_t(p))^2 dp}$$

where $\widehat{\text{ROC}}_t$ is the estimated ROC curve and ROC_t is the true curve for a given time point t . Figure 3 displays the RISE distribution for the time quantile 0.5 for different biomarker and event time distributions. The NPB method achieves lowest RISE values across all setups, indicating better performance in estimating the ROC curve. Methods like **survivalROC** (NNE and KM) and **timeROC** show higher RISE values, suggesting less precise estimates. Kernel-based methods such as **cenROC** and **smoothROctime** also perform well, but do not outperform NPB, particularly for more complex biomarker distributions like the normal mixture and chi-squared. Supplementary Figure 10 provides additional results for different sample sizes with a 50% censoring rate and a correlation of $\rho = -0.7$.

5.3. Conditional results

For the conditional case, we generated a continuous covariate from a standard uniform distribution $X \sim U(0, 1)$. To ensure consistency with the marginal distributions from the previously described unconditional data generating process and to incorporate the covariate shift on a standardized scale, we adjusted \mathbf{Z} to $(Z_1 + \gamma_Y X, Z_2 + \gamma_T X)$ where $\gamma_Y = 0.5$ and $\gamma_T = 3$. We then applied the standard normal CDF followed by the appropriate quantile function of the marginal distribution.

We compare our NPB approach to the only existing method for time-dependent ROC analysis with covariates that has available code. The R package **CondTimeROC** implements a non-parametric kernel smoothing technique for one continuous covariate (Rodríguez-Álvarez *et al.* 2016). There are several estimators implemented in the package: smooth with bandwidth selected using a plug-in approach (Altman and Leger 1995) or data-driven (Li *et al.* 2013) and completely nonparametric. The package also implements the semiparametric technique of Song and Zhou (2008).

For the various methods, we evaluated the covariate-specific ROC curve $\text{ROC}_t(x)$ at different values of the covariate using functional boxplots, shown in Figure 4. These plots summarize the ROC functions over 1000 replications. The dashed line represents the median function, the grey area highlights the 50% central region and the blue curves are analogous to whiskers in a traditional boxplot. The red curve represents the ROC curve from the true data-generating process. To ensure comparable sensitivity and specificity calculations across methods, we varied t based on covariates so that each analysis included an equal number of uncensored observations. This adjustment was necessary for the nonparametric methods, which had high variance when only a few data points were available for estimation. The NPB model estimates are unbiased and show low variance. In contrast, the ROC estimates from the smoothing method appear sensitive to the choice of bandwidth, leading to bias in some cases. The nonparametric estimates are unbiased but show high variability, while the semiparametric estimates are biased, likely due to the violation of the proportional hazards assumption.

We also evaluated the performance of parameter estimates from our NPB model in the presence of multiple covariates. For this, we generated two continuous covariates from a standard

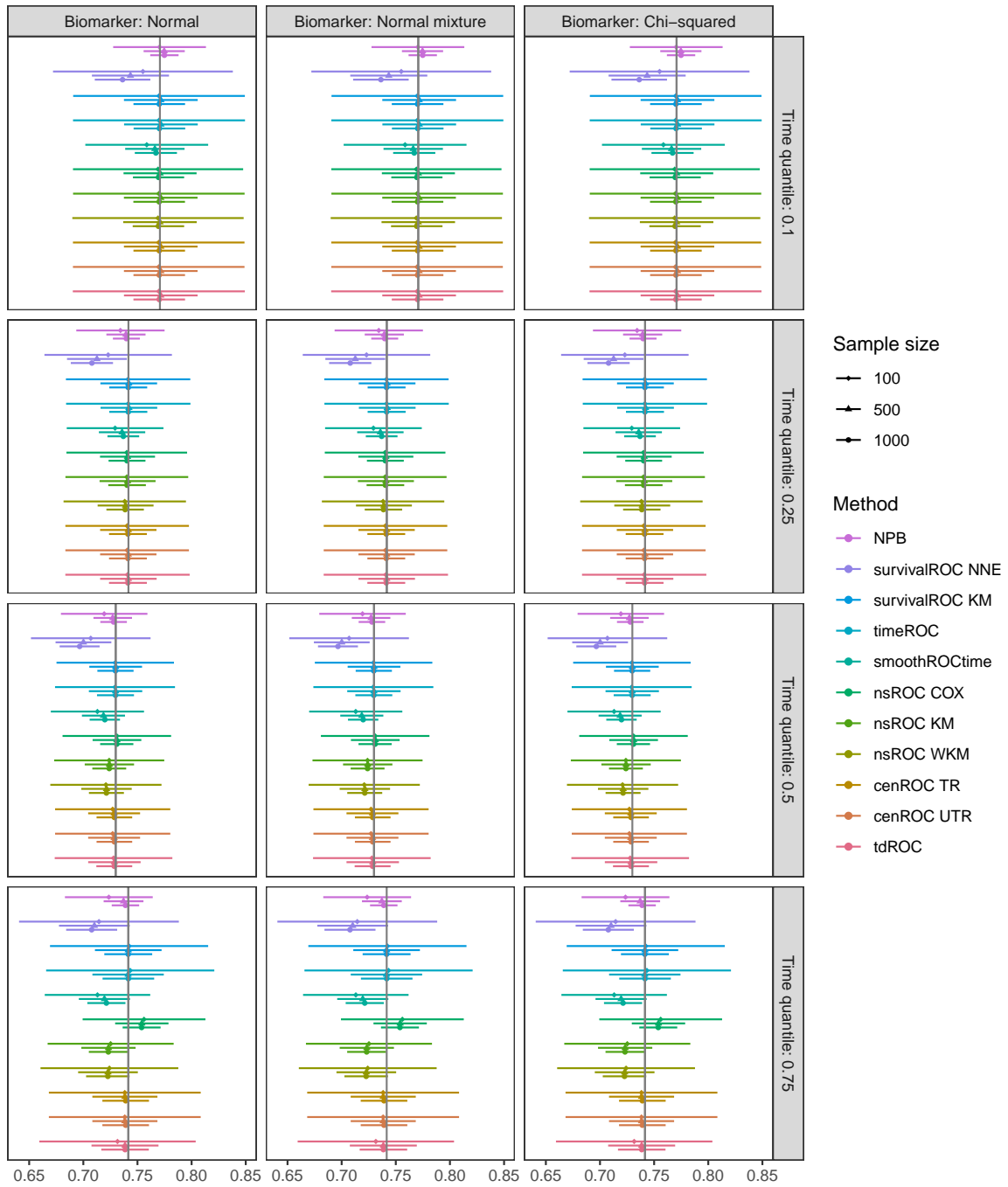


Figure 2: Mean and standard deviation of the unconditional AUC for each method with sample sizes of $N = \{100, 500, 1000\}$, Weibull event time distribution, 30% censoring rate and a correlation of $\rho = -0.5$ between transformed biomarker and event time distributions. The evaluation is across different biomarker distributions (Normal, Normal mixture, Chi-squared) and time quantiles (0.1, 0.25, 0.5, 0.75).

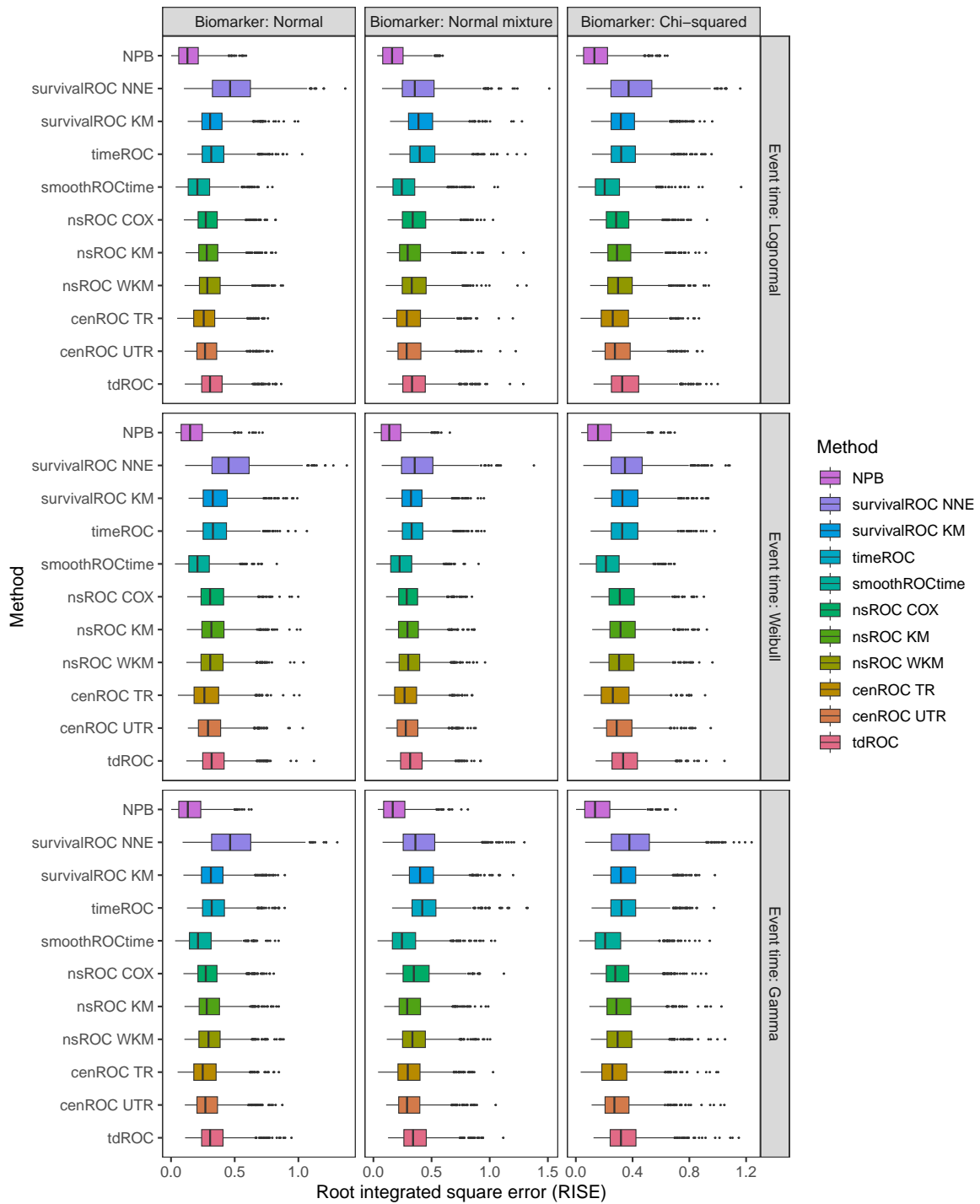


Figure 3: Distribution of root integrated squared errors (RISE) for unconditional ROC estimators at the median time quantile with a sample size of $N = 500$, event time distributions of $\{\text{Lognormal}, \text{Weibull}, \text{Gamma}\}$, 30% censoring rate and a correlation of $\rho = -0.5$ between transformed biomarker and event time distributions.

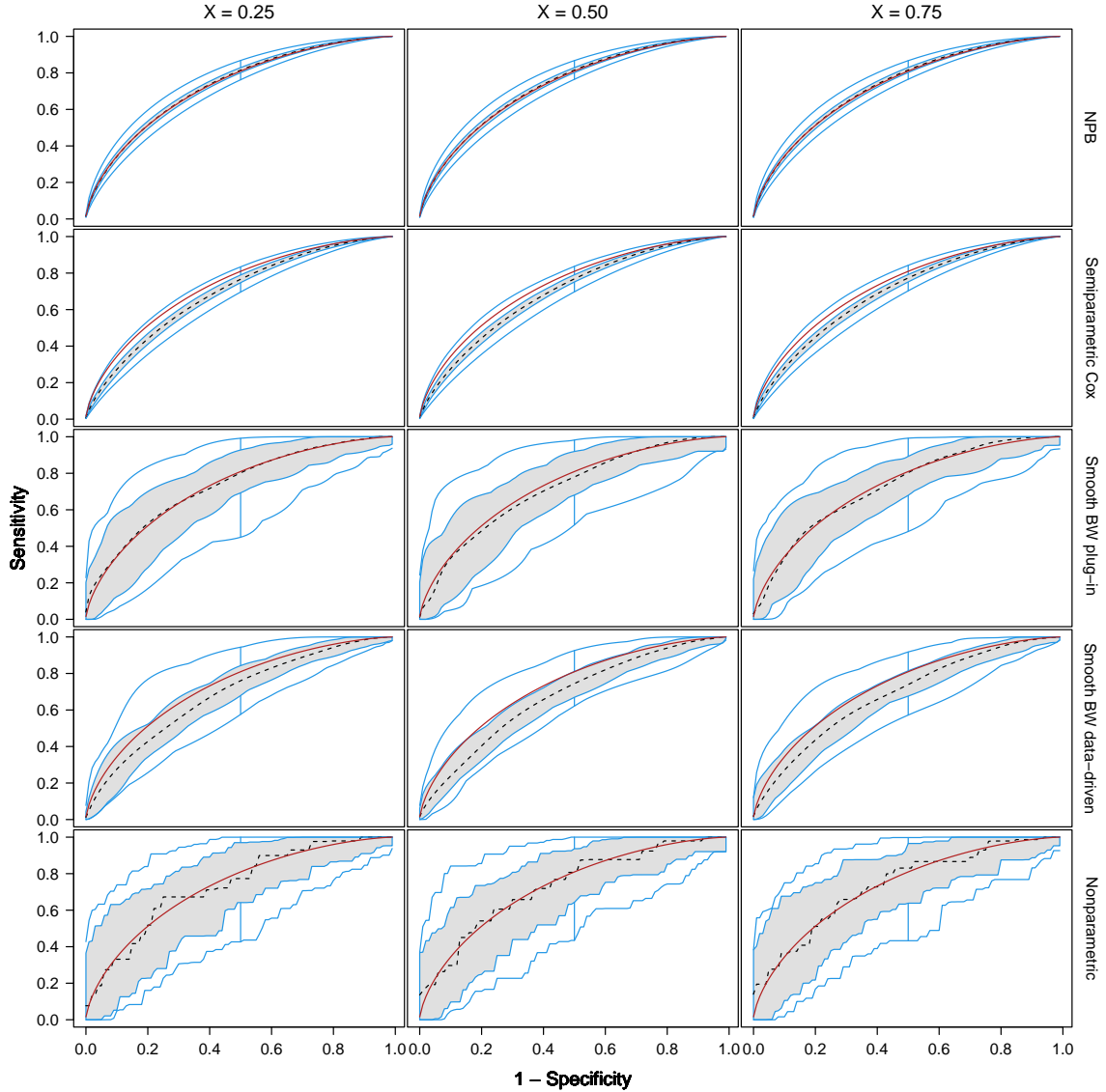


Figure 4: Functional boxplots for covariate-specific time dependent ROC curves at the median time quantile, with a sample size of $N = 500$, Weibull event time distribution, 30% censoring rate, and a correlation of $\rho = -0.5$ between transformed biomarker and event time distributions. The red line indicates the true covariate-specific ROC curve for each case.

uniform distribution and one binary covariate. Supplementary Figure 11 presents the bias of the parameter estimates under different sample sizes and censoring proportions. The results followed the same pattern as observed in previous settings. That is, the likelihood-based inference procedures produced unbiased and efficient estimates. However, it is important to note that when the dependency structure changes or when the covariates include nonlinear terms, the estimates can become biased. The performance of the NPB under model misspecification is evaluated in Supplementary Material B.2.

6. Application to prognostic biomarkers in ALS

In this section, we apply our framework to data from a study on prognostic biomarkers for ALS (Benatar *et al.* 2020), as detailed in Section 2. Serum NfL values in the current report were corrected for a 4-fold dilution factor that was inadvertently omitted in the previous publication. We apply the NPB model to determine the prognostic accuracy of baseline serum NfL concentration in predicting survival time in ALS. Our analysis begins with an unconditional model and we then incorporate baseline covariates to assess their impact on prognostic accuracy.

6.1. Unconditional NPB model

We estimated the unconditional NPB model to assess the prognostic accuracy of baseline NfL concentration for predicting survival time in ALS. Supplementary Figure 13 shows the modeled density which demonstrates a good fit to the observed data. The model captures the negative correlation between baseline NfL levels and survival time. The NPB model can then be used to generate the time-dependent ROC curve and all relevant summary indices, such as the AUC, Youden index (which lies between 0 and 1), optimal threshold, sensitivity, and specificity. The model-based summary statistics, along with their corresponding 95% confidence intervals are presented in Table 2. The optimal NfL threshold is defined as the value where sensitivity and specificity are maximized. The results indicate that the prognostic accuracy of baseline NfL in predicting survival over longer time horizons diminishes.

Time (months)	AUC (95% CI)	Youden index (95% CI)	Optimal threshold (95% CI)	Sensitivity (95% CI)	Specificity (95% CI)
3	0.78 (0.70, 0.86)	0.42 (0.29, 0.55)	92.93 (77.82, 108.04)	0.73 (0.66, 0.80)	0.69 (0.63, 0.76)
6	0.75 (0.68, 0.83)	0.37 (0.26, 0.49)	84.85 (72.50, 97.19)	0.71 (0.65, 0.78)	0.66 (0.61, 0.71)
12	0.71 (0.65, 0.78)	0.31 (0.21, 0.41)	76.77 (65.71, 87.83)	0.66 (0.60, 0.72)	0.65 (0.60, 0.70)
24	0.70 (0.63, 0.76)	0.28 (0.19, 0.38)	64.65 (55.38, 73.92)	0.65 (0.60, 0.70)	0.63 (0.58, 0.68)

Table 2: Model-based summary statistics describing the prognostic accuracy of baseline serum NfL concentration for predicting survival at different time points. The table includes the AUC, Youden index, optimal threshold for NfL concentration, sensitivity and specificity at the optimal threshold, each presented with their corresponding 95% confidence intervals (CI) at 3, 6, 12, and 24 months.

Access to the joint distribution allows us to estimate the survival time distribution for specific ranges of baseline NfL concentrations. NfL levels were categorized into tertiles (low, medium, high), as shown in Figure 5. The results depict an association between higher NfL levels and shorter survival times, with the highest tertile exhibiting the steepest decline in survival probability. The model also provides estimates for median survival time and other quantiles, showing that higher NfL levels predict shorter survival times across all quantiles. Additionally, the rate of decline in the post-ALSFRS-R score is strongly associated with ALS survival. Individuals with higher NfL levels exhibit a more rapid decline in ALSFRS-R scores, as shown in Supplementary Figure 14.

6.2. Conditional NPB model

While the unconditional model provides an overall view of the relationship between NfL and

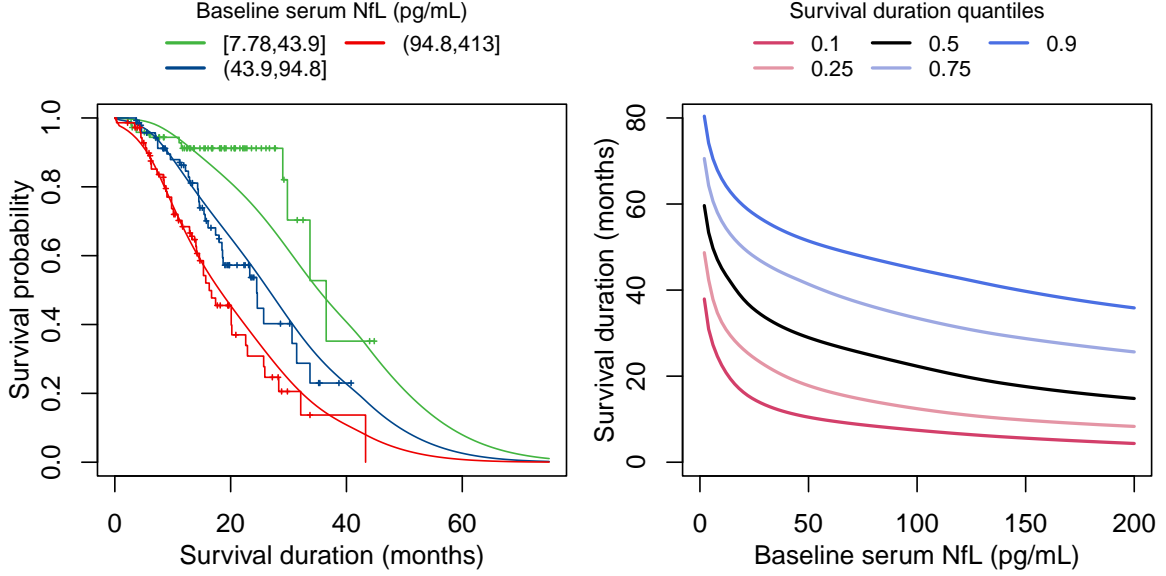


Figure 5: Left: Survival curves stratified by tertiles of baseline serum neurofilament light (NfL) concentration. Right: Survival time quantiles as a function of baseline serum NfL concentration.

survival, incorporating covariates allows us to account for confounding effects and assess how these factors influence the prognostic accuracy of NfL. We considered several baseline factors that could influence the prognostic accuracy of NfL for ALS.

The mean baseline age of patients was 60.1 years (SD 11.7). The cohort comprised 93 females (42.7%) and 125 males (57.3%). In terms of genetic characteristics, the C9orf72 repeat expansion was present in 24 participants (11.0%) and absent in 194 patients (89.0%). Site of symptom onset was bulbar only for 42 participants (19.3%), limb only for 154 (70.6%), and other regions or multi-region for 22 (10.0%). The median baseline ALS Functional Rating Scale – Revised (ALSFRS-R) score was 36.0 points (IQR 9.0). We also assessed the past (i.e. pre-baseline) rate of disease progression, defined by

$$\Delta\text{FRS} = \frac{48 - \text{ALSFRS-R}_{\text{baseline}}}{\text{Months from onset to baseline}},$$

where 48 is the maximum score on the ALSFRS-R. The average ΔFRS was 0.60 points per month (SD 0.47).

For ease of the following visualizations, we fixed continuous variables to their mean values and categorical variables to their modal values, unless otherwise specified. We fit the conditional NPB model with the marginal model for NfL specified as

$$h_Y(Y_i | \boldsymbol{\vartheta}) = \beta_{Y,1}\text{Age}_i + f\beta_{Y,2}\text{Sex}_i + \beta_{Y,3}\text{C9}_i + \beta_{Y,4}\Delta\text{FRS}_i + \beta_{Y,5}\text{ALSF}_i + \beta_{Y,6}\text{Site}_i + Z$$

where the baseline transformation function is given by $h_Y(y | \boldsymbol{\vartheta}) = \sum_{m=0}^6 \vartheta_{Y,m} b_m(\log(y))$ and $Z \sim N(0, 1)$. The model for survival time includes the same covariates and the marginal transformation function follows a similar form. A plot of the estimated baseline transforma-

tion functions is provided in Supplementary Figure 15, showing the need for transformation in both NfL and survival time data.

The coefficients of the joint model are presented in Table 3. The unconditional correlation indicates whether there is a significant association between the biomarker and event time. If the confidence interval for this correlation includes zero, the biomarker likely lacks prognostic accuracy. For NfL, the unconditional correlation coefficient is relatively strong at -0.429 , with a 95% confidence interval of -0.283 to -0.547 , indicating a significant association with survival duration. The conditional correlation shows a reduction compared to the unconditional correlation, suggesting that some of the covariates account for a portion of the variation in survival duration.

Variable	NfL		Survival time	
	Coefficient (95% CI)			
Unconditional correlation	$-0.428 (-0.283, -0.547)$			
Conditional correlation	$-0.324 (-0.149, -0.471)$			
Covariates β_i				
Age	0.020 (0.010, 0.031)	$-0.021 (-0.036, -0.006)$	
Sex - Male	0.565 (0.290, 0.840)	$0.142 (-0.239, 0.522)$	
C9orf72 - Positive	0.389 ($-0.055, 0.833$)	$-0.541 (-1.076, -0.006)$	
Δ FRS	0.801 (0.467, 1.135)	$-0.513 (-0.885, -0.142)$	
Baseline ALSFRS-R	0.000 ($-0.021, 0.021$)	$0.035 (0.015, 0.054)$	
Site - Bulbar only	0.700 (0.284, 1.116)	$-0.282 (-0.721, 0.157)$	
Site - Other	0.284 ($-0.129, 0.697$)	$0.649 (-0.067, 1.366)$	

Table 3: Estimated coefficients of the nonparanormal prognostic biomarker model along with their corresponding 95% confidence intervals (CI).

Figure 6 shows the estimated joint distribution of baseline NfL concentration and survival time by the site of ALS onset. In both groups, higher baseline NfL concentrations are generally associated with shorter survival times. Patients with bulbar-onset ALS show lower survival times and higher NfL concentrations compared to those with limb-onset ALS. This aligns with previous research, which suggests that bulbar-onset ALS typically has a more aggressive disease progression (Zoccolella *et al.* 2008).

Figure 7 shows the estimated age-specific time-dependent ROC curves. The accuracy of baseline NfL in predicting survival declines as the time horizon increases. For any given time horizon, the prognostic accuracy of NfL decreases with increasing age. Further, age appears to have a greater impact when predicting early ALS prognosis compared to later stages of the disease.

The effect of different covariate combinations on prognostic accuracy varies, making it challenging to summarize these effects with a single model-based statistic or covariate-specific ROC curves. Figure 8 shows a spaghetti plot, where each line represents the time-dependent AUC for an individual patient's unique combination of covariates. The red line shows the smoothed average across all patients, while the blue line corresponds to the AUC from the unconditional model. Even after adjusting for covariates, the prognostic accuracy of baseline NfL declines over longer time horizons. However, incorporating covariates reduces the

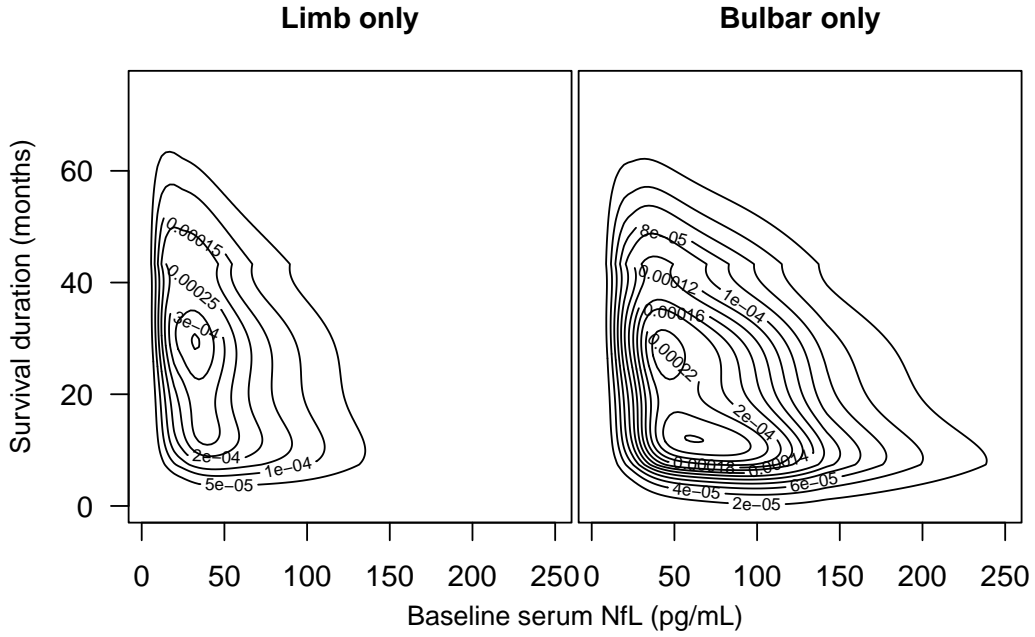


Figure 6: Bivariate density of baseline serum neurofilament light (NfL) concentration and survival time by the presence of the site of onset (limb only vs. bulbar only). The plot is based fixed covariate values for a 60-year-old male with a negative C9orf72 status, a progression rate (Δ FRS) of 0.60 points/month and a baseline ALSFRS-R score of 35.

prognostic accuracy of NfL. Failing to account for these factors may lead to overly optimistic estimates.

Model assessment can be found in Supplementary Figure 16. The spline term for baseline NfL plotted against survival time shows a monotonically decreasing trend, indicating that the model's assumptions hold.

7. Extensions

Observational studies often involve additional complexities that need to be addressed for accurate analysis of prognostic biomarkers. These may include issues such as limits of detection in biomarker measurements, non-independent censoring times, covariate-driven dependencies between the biomarker and event time, and the potential presence of nonlinear covariate effects. We did not investigate these in the ALS case study we analyzed, but our NPB framework can be extended to accommodate these scenarios. We detail these briefly in this section.

7.1. Limit of detection in biomarkers

Biomarker measurements are often affected by random errors and limits of detection issues. Ignoring of such a data characteristic can reduce the biomarker's prognostic accuracy. Statis-

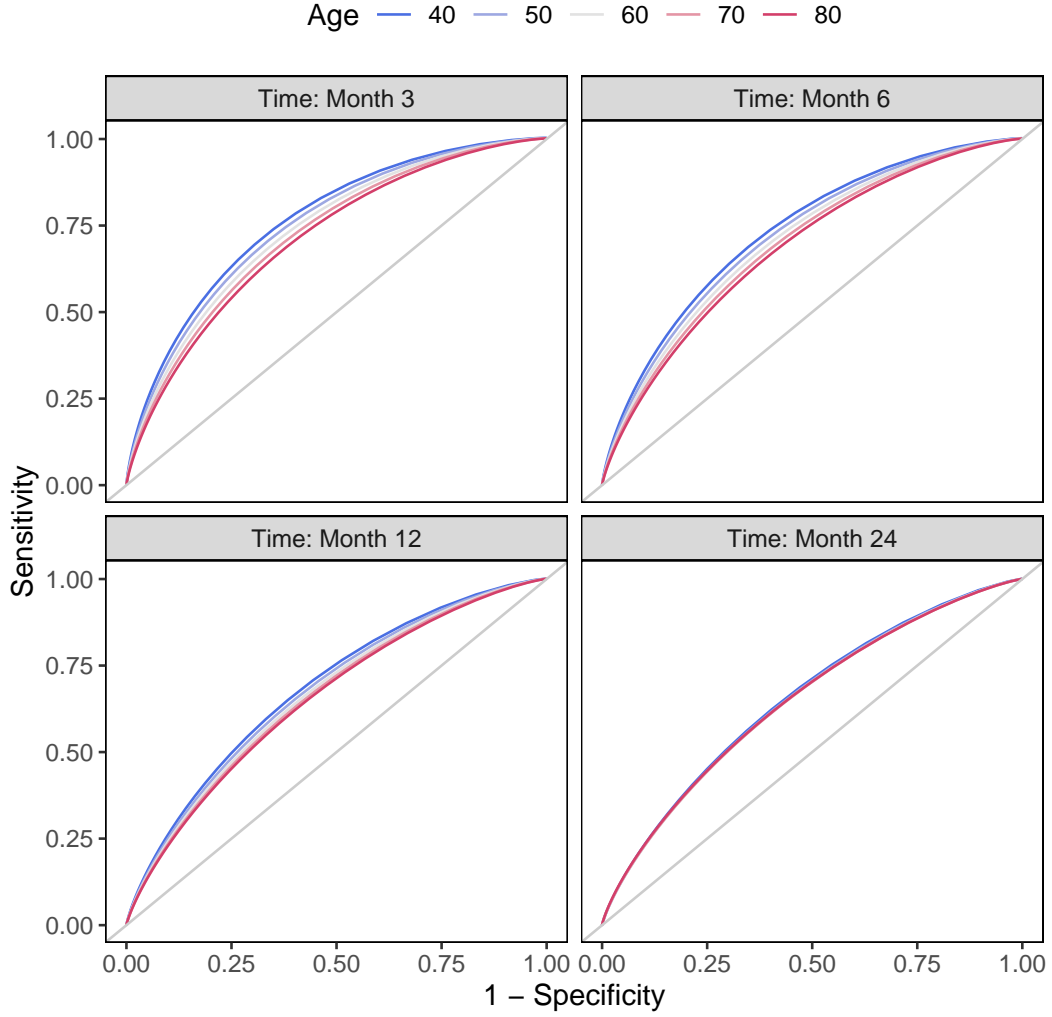


Figure 7: Covariate-specific time-dependent ROC curves by age and the presence of the C9orf72 repeat expansion for a female with a ΔFRS of 0.5. The plot is based fixed covariate values for a male with a negative C9orf72 status, a progression rate (ΔFRS) of 0.60 points/month and a baseline ALSFRS-R score of 35.

tically, this is a form of interval censoring where measurements below the detection limit are left-censored and those above the detection limit are right-censored. In the NPB framework, the likelihood can be adjusted to account for this censoring in the biomarker data. For independent interval-censored biomarker measurements and interval-censored event times, we observe $O_i = (\underline{y}_i, \bar{y}_i, \underline{t}_i, \bar{t}_i, \mathbf{x}_i)$ and the likelihood contribution is expressed as

$$\begin{aligned} \ell_c(\boldsymbol{\theta} \mid O_i) &= F(\bar{y}_i, \bar{t}_i \mid \mathbf{x}_i) - F(\underline{y}_i, \underline{t}_i \mid \mathbf{x}_i) \\ &= \int_{h_Y(\underline{y}_i \mid \vartheta_Y)}^{h_Y(\bar{y}_i \mid \vartheta_Y)} \int_{h_T(\underline{t}_i \mid \vartheta_T)}^{h_T(\bar{t}_i \mid \vartheta_T)} \phi_\rho \left(z_Y - \mathbf{x}_i^\top \boldsymbol{\beta}_Y, z_T - \mathbf{x}_i^\top \boldsymbol{\beta}_T \right) dz_Y dz_T. \end{aligned}$$

In this formulation, lower detection limits are treated as a special case where $\underline{y}_i = -\infty$ and upper detection limits are treated as $\bar{y}_i = \infty$. Inference can subsequently proceed as detailed

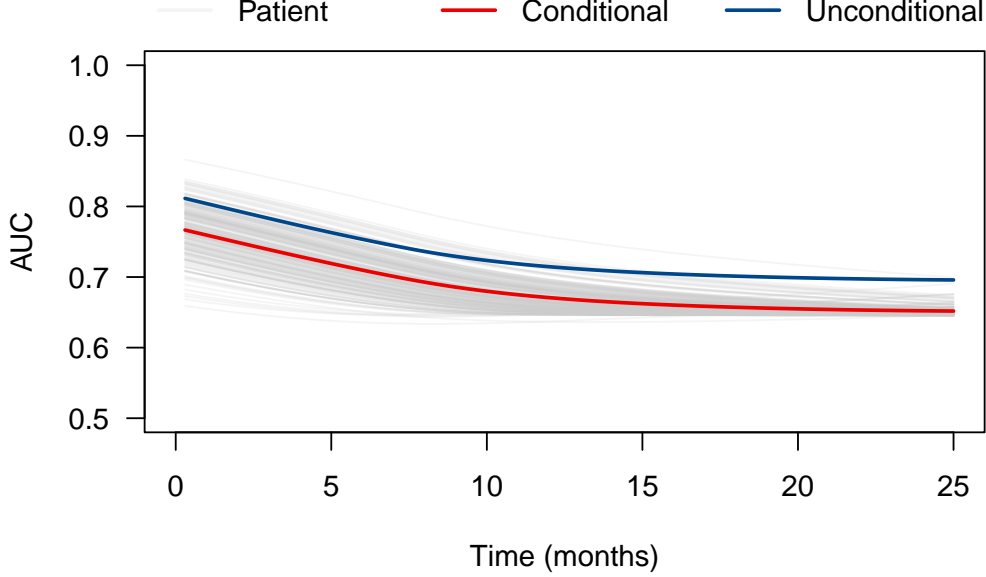


Figure 8: Spaghetti plot for patient-specific time-dependent AUCs (in gray), smoothed average across all patients (red) and unconditional (blue).

previously and the resulting estimates would not suffer from the negative bias of ignoring the true nature of the biomarker measurement.

7.2. Dependent censoring

In the methods presented above, we assumed conditionally independent censoring. That is, once the covariates \mathbf{X} are known, the event time T and censoring time C are independent, i.e., $T \perp\!\!\!\perp C \mid \mathbf{X} = \mathbf{x}$. However, this assumption may not hold in practice. Event time can influence censoring time and censoring may depend on biomarker levels. For example, in ALS, elevated levels of NfL might be associated with a higher risk of death, leading to study dropout as patients become too sick for follow-up.

To address this, the NPB framework can be extended to model the joint relationship between Y , T , and C given $\mathbf{X} = \mathbf{x}$, allowing for non-independent censoring. Under certain conditions, such a model is identifiable when the marginal distributions of T and C are parametrically specified, for example, as log-normal or Weibull distributions (Czado and Van Keilegom 2023). Alternatively, the event time can be modeled semiparametrically with a Cox proportional hazards model while censoring times follow a Weibull model (Deresa and Van Keilegom 2024). From any such trivariate model, we can derive the bivariate distribution of $(Y, T) \mid \mathbf{X} = \mathbf{x}$ using the Gaussian copula, now parameterized by a correlation matrix rather than a single parameter. The multivariate normal distribution’s properties allow us to subset the rows and columns of the correlation matrix related to Y and T , and proceed with calculating cumulative sensitivity and dynamic specificity as in the original model.

7.3. Covariate dependent correlation

In some medical conditions, the correlation between a biomarker and event time can vary based on covariates. For example, in ALS, the correlation between NfL levels and survival duration may depend on covariates such as age or disease onset site. Younger patients with limb-onset ALS might exhibit a weaker correlation between NfL and survival, whereas older patients or those with bulbar-onset ALS may show a stronger correlation due to faster disease progression.

In the NPB framework, the correlation matrix Σ can vary with the covariates \mathbf{x} , allowing the dependence structure between Y and T to change as a function of \mathbf{x} . For the bivariate case, the correlation between Y and T for a given set of covariates \mathbf{x} is given by

$$\rho(\mathbf{x}) = \frac{-\lambda(\mathbf{x})}{\sqrt{\lambda(\mathbf{x})^2 + 1}},$$

where $\lambda(\mathbf{x}) = \alpha + \mathbf{x}^\top \boldsymbol{\gamma}$ is one possible parameterization of the coefficient of the inverse Cholesky factor (Klein *et al.* 2022; Barratt and Boyd 2023). This flexibility in the correlation structure enables the model to capture covariate-dependent relationships between the biomarker and event time.

7.4. Alternative marginal models

The assumption of probit semiparametric transformation models can also be relaxed. An alternative approach is to use a continuous odds logistic regression model for the biomarker, known for its robustness properties (Harrell 2015; Sewak and Hothorn 2023), alongside a proportional hazards model for the event time

$$F_Y(y | \mathbf{x}) = \text{expit} \left(h_Y(y) - \mathbf{x}^\top \boldsymbol{\beta}_Y \right) \text{ and } F_T(t | \mathbf{x}) = 1 - \exp \left(- \exp \left(h_T(t) - \mathbf{x}^\top \boldsymbol{\beta}_T \right) \right).$$

In general, any absolutely continuous cumulative distribution function with a log-concave density can be substituted for the probit link function, providing flexibility in marginal model choice.

7.5. Nonlinear covariate modeling

The linear predictor in our marginal models may be insufficient to fully capture the effects of covariates in some cases. To address this, we can incorporate covariates directly into the multivariate NPB modeling framework by estimating the joint distribution of (Y, T, \mathbf{X}) using the parameterizations and estimation procedures described in Hothorn (2024b). This aligns to the approach of Rodríguez-Álvarez *et al.* (2016) but can be extended to incorporate multiple covariates. Continuous covariates can be parameterized using any polynomial or spline basis. To generate covariate-specific time-dependent ROC curves, we can determine the conditional distribution of $(Y, T) | \mathbf{X} = \mathbf{x}$ from the Gaussian copula.

8. Conclusion

In this paper, we present a statistical framework for evaluating the prognostic accuracy of biomarkers across different time horizons while accounting for patient characteristics. Using

covariate-specific sensitivity and specificity, we construct ROC curves and related summary indices to form the basis of our evaluation. The NPB model is built on two key components: (1) the Gaussian copula, which captures the dependence between the biomarker and event time, and (2) marginal models which incorporate the effects of covariates. The framework allows a broad class of functions to be fit to the data and can handle right and interval censoring. Our simulation studies demonstrate that the method performs well, yielding unbiased and efficient estimates. We anticipate the application of this approach in clinical trials focused on identifying new biomarkers for diseases such as ALS or in the development of new treatments where biomarkers could be used to stratify patients into subgroups based on their risk profiles.

8.1. Areas of future research

Several areas warrant further research. As with any joint modeling approach, the validity of the results depends on how well the assumed dependence structure captures the relationship between Y and T . If the Gaussian copula does not adequately model this dependence, it may lead to biased estimates. Our simulation study using an alternative dependence structure (Supplementary Figure 12) showed that while the NPB model performs well under correlation-driven dependence, it struggles when Y and T follow a strong, direct functional relationship.

To address this, we introduce a model assessment technique to evaluate the suitability of the Gaussian copula, which was confirmed to hold in our application example. However, alternative copula choices or more flexible dependence structures could further improve the method. Ultimately, method selection involves a bias-variance trade-off: model-based approaches offer low variance but can be biased under misspecification, while fully nonparametric methods are asymptotically unbiased but prone to high variability and limited to single continuous covariates. Future work could explore hybrid approaches that balance these two more effectively, ensuring mostly unbiased estimates while accommodating complex dependence structures.

The use of a linear predictor for covariates was selected for simplicity, though the proposed model extensions provide flexibility by relaxing this assumption as needed. Also, while our method can accommodate a proportional hazards model if suitable for a given dataset, it is not restricted to this approach, allowing for broader applicability within the framework. Another area for development is covariate selection; though out-of-sample log-likelihoods could be employed to identify key covariates, this approach is computationally intensive and often requires large datasets. Our goal is to offer a framework that enables practitioners to select covariates based on clinical knowledge, reducing the need of computationally demanding techniques.

8.2. Prognostic accuracy of NfL

Adjusting for covariates is essential in accurately assessing the prognostic accuracy of NfL. Without accounting for patient characteristics, the prognostic value of NfL may be overestimated. We observed that NfL's prognostic accuracy is lower in patients with poor prognostic factors such as older age, C9orf72-positive status and higher Δ FRS values. Interestingly, factors such as sex, site of onset, and baseline ALSFRS-R score had minimal impact on the prognostic accuracy of NfL.

In our study, we focused on the prognostic accuracy of baseline biomarker measurements.

However, many biomarkers, including those used in ALS, are measured longitudinally. Extending the model to incorporate repeated biomarker measurements over time would be an important area of future research. Additionally, exploring optimal combinations of biomarkers and covariates for improved prognostic accuracy represents a promising direction for further study. Note that although we applied our method to ALS, the proposed NPB framework is broadly applicable to prognostic biomarkers across various medical conditions.

As the discovery of new biomarkers continues to grow, it becomes increasingly important to have methods to evaluate their prognostic accuracy. Our approach provides a flexible solution that allows for the identification of more homogeneous patient populations based on covariate-specific biomarker performance. In turn, this comes with the potential to reduce the required sample size in clinical trials, making studies more efficient and cost-effective.

Computational details

We used **mvtnorm** (Genz *et al.* 2025, version 1.3.3) to sample from multivariate normal distributions, **pracma** (Borchers 2023, version 2.4.4) for numerical integration of ROC curves, and **qrng** (Hofert and Lemieux 2024, version 0.0.10) for random number generation. Furthermore, we used **tramME** (Tamasi 2024, version 1.0.7) for estimating conditional distributions.

To evaluate competitor methods in our simulation studies, we used the following R packages: **survivalROC** (Heagerty and Saha-Chaudhuri 2022, version 1.0.3.1) for nearest-neighbor and Kaplan-Meier estimations; **timeROC** (Blanche *et al.* 2013a, version 0.4) for inverse probability weighting; **smoothROctime** (Diaz-Coto 2018, version 0.1.0) for bivariate kernel density estimation; **nsROC** (Fernandez 2018, version 1.1) for proportional hazards-based methods; **cenROC** (Beyene and El Ghouh 2023, version 2.0.0) for smoothed kernel methods; **tdROC** (Li *et al.* 2023, version 2.0) for nonparametric kernel smoothing weights. Each package was used to implement its respective method for estimating time-dependent ROC curves.

All computations were performed using R version 4.4.2 (R Core Team 2024).

A reference implementation of the nonparanormal prognostic biomarker model is available in the **tram** add-on package (Hothorn *et al.* 2025) to the R system for statistical computing. The simulation results presented in Sections 5 are available on <https://gitlab.com/asewak/npb>. The application to prognostic biomarkers in ALS in Section 6 can be reproduced by running the code from within R:

```
install.packages("tram")
library("tram")
demo("npb", package = "tram")
```

Acknowledgements

Torsten Hothorn received financial support from the Swiss National Science Foundation (grant number 200021_219384).

References

- Altman N, Leger C (1995). “Bandwidth Selection for Kernel Distribution Function Estimation.” *Journal of Statistical Planning and Inference*, **46**(2), 195–214. doi:10.1016/0378-3758(94)00102-2.
- Bansal A, Heagerty PJ (2019). “A Comparison of Landmark Methods and Time-Dependent ROC Methods to Evaluate the Time-Varying Performance of Prognostic Markers for Survival Outcomes.” *Diagnostic and Prognostic Research*, **3**, 1–13. doi:10.1186/s41512-019-0057-6.
- Barratt S, Boyd S (2023). “Covariance Prediction via Convex Optimization.” *Optimization and Engineering*, **24**(3), 2045–2078. doi:10.1007/s11081-022-09765-w.
- Benatar M, Macklin EA, Malaspina A, Rogers ML, Hornstein E, Lombardi V, Renfrey D, Shephard S, Magen I, Cohen Y, Granit V, Statland JM, Heckmann JM, Rademakers R, McHutchison CA, Petrucelli L, McMillan CT, Wu J, CReATe Consortium PGB1 Study Investigators (2024). “Prognostic Clinical and Biological Markers for Amyotrophic Lateral Sclerosis Disease Progression: Validation and Implications for Clinical Trial Design and Analysis.” *eBioMedicine*, **108**, 105323. doi:10.1016/j.ebiom.2024.105323.
- Benatar M, Wu J, Turner MR (2023). “Neurofilament Light Chain in Drug Development for Amyotrophic Lateral Sclerosis: A Critical Appraisal.” *Brain*, **146**(7), 2711–2716. doi:10.1093/brain/awac394.
- Benatar M, Zhang L, Wang L, Granit V, Statland J, Barohn R, Swenson A, Ravits J, Jackson C, Burns TM, Trivedi J, Piro EP, Caress J, Katz J, McCauley JL, Rademakers R, Malaspina A, Ostrow LW, Wu J, Hussain S, Cooley A, Li Y, Wallace M, Steele J, Hernandez JP, Medina J, Paredes ME, Manso A, Ravelo N, Levy W, Whitehead P, Zuchner S, Pasnoor M, Jawdat O, Jabari D, Farmakidis C, Glenn M, Dimachkie MM, Herbelin L, Tanui H, Anderson S, Walker M, Liu T, McCally A, Heim A, Currence M, Harness Y, Sieren J, Gibson E, Gutierrez G, Bussey D, Previte R, Kittrell P, Joshi A, Conger A, Hastings D, Caristo I, Marandi M, Carty S, Taylor JP, Wu G, Rampersaud E, Schule R, van Blitterswijk M (2020). “Validation of Serum Neurofilaments As Prognostic and Potential Pharmacodynamic Biomarkers for ALS.” *Neurology*, **95**(1), e59–e69. doi:10.1212/wnl.0000000000009559.
- Beyene KM, Chen DG (2024). “Time-Dependent Receiver Operating Characteristic Curve Estimator for Correlated Right-Censored Time-To-Event Data.” *Statistical Methods in Medical Research*, **33**(1), 162–181. doi:10.1177/09622802231220496.
- Beyene KM, El Ghouh A (2020). “Smoothed Time-Dependent Receiver Operating Characteristic Curve for Right Censored Survival Data.” *Statistics in Medicine*, **39**(24), 3373–3396. doi:10.1002/sim.8671.
- Beyene KM, El Ghouh A (2023). *cenROC: Estimating Time-Dependent ROC Curve and AUC for Censored Data*. doi:10.32614/CRAN.package.cenROC. R package version 2.0.0.

- Blanche P, Dartigues JF, Jacqmin-Gadda H (2013a). “Estimating and Comparing Time-Dependent Areas under Receiver Operating Characteristic Curves for Censored Event Times with Competing Risks.” *Statistics in Medicine*, **32**(30), 5381–5397. doi:10.1002/sim.5958.
- Blanche P, Dartigues JF, Jacqmin-Gadda H (2013b). “Review and Comparison of ROC Curve Estimators for a Time-Dependent Outcome with Marker-Dependent Censoring.” *Biometrical Journal*, **55**(5), 687–704. doi:10.1002/bimj.201200045.
- Borchers HW (2023). *pracma: Practical Numerical Math Functions*. doi:10.32614/CRAN.package.pracma. R package version 2.4.4.
- Cai T, Pepe MS, Zheng Y, Lumley T, Jenny NS (2006). “The Sensitivity and Specificity of Markers for Event Times.” *Biostatistics*, **7**(2), 182–197. doi:10.1093/biostatistics/kxi047.
- Cox DR (1972). “Regression Models and Life-Tables.” *Journal of the Royal Statistical Society: Series B (Methodological)*, **34**(2), 187–202. doi:/10.1111/j.2517-6161.1972.tb00899.x.
- Czado C, Van Keilegom I (2023). “Dependent Censoring Based on Parametric Copulas.” *Biometrika*, **110**(3), 721–738. doi:10.1093/biomet/asac067.
- Deresa NW, Van Keilegom I (2024). “Copula Based Cox Proportional Hazards Models for Dependent Censoring.” *Journal of the American Statistical Association*, **119**(546), 1044–1054. doi:10.1080/01621459.2022.2161387.
- Dette H, Van Hecke R, Volgushev S (2014). “Some Comments on Copula-Based Regression.” *Journal of the American Statistical Association*, **109**(507), 1319–1324. doi:10.1080/01621459.2014.916577.
- Dey R, Hanley JA, Saha-Chaudhuri P (2023). “Inference for Covariate-adjusted Time-dependent Prognostic Accuracy Measures.” *Statistics in Medicine*, **42**(23), 4082–4110. doi:10.1002/sim.9848.
- Diaz-Coto S (2018). *smoothROctime: Smooth Time-Dependent ROC Curve Estimation*. doi:10.32614/CRAN.package.smoothROctime. R package version 0.1.0.
- Escarela G, Vásquez AR, González-Farías G, Márquez-Urbina JU (2023). “Copula Modeling for the Estimation of Measures of Marker Classification and Predictiveness Performance with Survival Outcomes.” *Statistical Methods in Medical Research*, **32**(6), 1203–1216. doi:10.1177/09622802231167588.
- Etzioni R, Pepe M, Longton G, Hu C, Goodman G (1999). “Incorporating the Time Dimension in Receiver Operating Characteristic Curves: A Case Study of Prostate Cancer.” *Medical Decision Making*, **19**(3), 242–251. doi:10.1177/0272989x9901900303.
- Farouki RT (2012). “The Bernstein Polynomial Basis: A Centennial Retrospective.” *Computer Aided Geometric Design*, **29**(6), 379–419. doi:10.1016/j.cagd.2012.03.001.
- Feldman EL, Goutman SA, Petri S, Mazzini L, Savelieff MG, Shaw PJ, Sobue G (2022). “Amyotrophic Lateral Sclerosis.” *The Lancet*, **400**(10360), 1363–1380. doi:10.1016/s0140-6736(22)01272-7.

- Fernandez SP (2018). *nsROC: Non-Standard ROC Curve Analysis*. doi:10.32614/CRAN.package.nsROC. R package version 1.1.
- Genz A (1992). “Numerical Computation of Multivariate Normal Probabilities.” *Journal of Computational and Graphical Statistics*, **1**(2), 141–149. doi:10.2307/1390838.
- Genz A, Bretz F, Miwa T, Mi X, Hothorn T (2025). *mvtnorm: Multivariate Normal and t Distributions*. doi:10.32614/CRAN.package.mvtnorm. R package version 1.3-3.
- Harrell Jr FE (2015). “Ordinal Logistic Regression.” In *Regression Modeling Strategies*, pp. 311–325. Springer. doi:10.1007/978-3-319-19425-7_13.
- Heagerty PJ, Lumley T, Pepe MS (2000). “Time-Dependent ROC Curves for Censored Survival Data and a Diagnostic Marker.” *Biometrics*, **56**(2), 337–344. doi:10.1111/j.0006-341x.2000.00337.x.
- Heagerty PJ, Saha-Chaudhuri P (2022). *survivalROC: Time-Dependent ROC Curve Estimation from Censored Survival Data*. doi:10.32614/CRAN.package.survivalROC. R package version 1.0.3.1.
- Heagerty PJ, Zheng Y (2005). “Survival Model Predictive Accuracy and ROC Curves.” *Biometrics*, **61**(1), 92–105. doi:10.1111/j.0006-341x.2005.030814.x.
- Hofert M, Lemieux C (2024). *qrng: (Randomized) Quasi-Random Number Generators*. doi:10.32614/CRAN.package.qrng. R package version 0.0-10.
- Hothorn T (2024a). *Multivariate Normal Log-likelihoods in the mvtnorm Package*. doi:10.32614/CRAN.package.mvtnorm. R package vignette version 1.3-0.
- Hothorn T (2024b). “On Nonparanormal Likelihoods.” doi:10.48550/arXiv.2408.17346. arXiv:2408.17346 [stat.ME].
- Hothorn T, Barbanti L, Siegfried S, Kook L (2025). *tram: Transformation Models*. doi:10.32614/CRAN.package.tram. R package version 1.2-1.
- Hothorn T, Möst L, Bühlmann P (2018). “Most Likely Transformations.” *Scandinavian Journal of Statistics*, **45**(1), 110–134. doi:10.1111/sjos.12291.
- Janes H, Pepe MS (2008). “Adjusting for Covariates in Studies of Diagnostic, Screening, or Prognostic Markers: An Old Concept in a New Setting.” *American Journal of Epidemiology*, **168**(1), 89–97. doi:10.1093/aje/kwn099.
- Jiang X, Li W, Li R, Ning J (2024). “Addressing Subject Heterogeneity in Time-dependent Discrimination for Biomarker Evaluation.” *Statistics in Medicine*, **43**(7), 1341–1353. doi:10.1002/sim.10024.
- Kamarudin AN, Cox T, Kolamunnage-Dona R (2017). “Time-Dependent ROC Curve Analysis in Medical Research: Current Methods and Applications.” *BMC Medical Research Methodology*, **17**, 1–19. doi:10.1186/s12874-017-0332-6.

- Kiernan MC, Vucic S, Talbot K, McDermott CJ, Hardiman O, Shefner JM, Al-Chalabi A, Huynh W, Cudkovic M, Talman P, Van den Berg LH, Dharmadasa T, Wicks P, Reilly C, Turner MR (2021). “Improving Clinical Trial Outcomes in Amyotrophic Lateral Sclerosis.” *Nature Reviews Neurology*, **17**(2), 104–118. doi:10.1038/s41582-020-00434-z.
- Klein N, Hothorn T, Barbanti L, Kneib T (2022). “Multivariate Conditional Transformation Models.” *Scandinavian Journal of Statistics*, **49**, 116–142. doi:10.1111/sjos.12501.
- Koini M, Pirpamer L, Hofer E, Buchmann A, Pinter D, Ropele S, Enzinger C, Benkert P, Leppert D, Kuhle J, Schmidt R, Khalil M (2021). “Factors Influencing Serum Neurofilament Light Chain Levels in Normal Aging.” *Ageing*, **13**(24), 25729. doi:10.18632/aging.203790.
- Lambert J, Chevret S (2016). “Summary Measure of Discrimination in Survival Models Based on Cumulative/dynamic Time-Dependent ROC Curves.” *Statistical Methods in Medical Research*, **25**(5), 2088–2102. doi:10.1177/0962280213515571.
- Le Borgne F, Combescure C, Gillaizeau F, Giral M, Chapal M, Giraudeau B, Foucher Y (2018). “Standardized and weighted time-dependent receiver operating characteristic curves to evaluate the intrinsic prognostic capacities of a marker by taking into account confounding factors.” *Statistical Methods in Medical Research*, **27**(11), 3397–3410. doi:10.1177/0962280217702416.
- Li L, Greene T, Hu B (2018). “A Simple Method to Estimate the Time-Dependent Receiver Operating Characteristic Curve and the Area under the Curve with Right Censored Data.” *Statistical Methods in Medical Research*, **27**(8), 2264–2278. doi:10.1177/0962280216680239.
- Li Q, Lin J, Racine JS (2013). “Optimal Bandwidth Selection for Nonparametric Conditional Distribution and Quantile Functions.” *Journal of Business & Economic Statistics*, **31**(1), 57–65. doi:10.1080/07350015.2012.738955.
- Li S, Ning Y (2015). “Estimation of Covariate-Specific Time-Dependent ROC Curves in the Presence of Missing Biomarkers.” *Biometrics*, **71**(3), 666–676. doi:10.1111/biom.12312.
- Li X, Yin Z, Li L (2023). *tdROC: Nonparametric Estimation of Time-Dependent ROC, Brier Score, and Survival Difference from Right Censored Time-to-Event Data with or without Competing Risks*. doi:10.32614/CRAN.package.tdROC. R package version 2.0.
- Liu H, Lafferty J, Wasserman L (2009). “The Nonparanormal: Semiparametric Estimation of High Dimensional Undirected Graphs.” *Journal of Machine Learning Research*, **10**(80), 2295–2328. URL <http://jmlr.org/papers/v10/liu09a.html>.
- Lu CH, Macdonald-Wallis C, Gray E, Pearce N, Petzold A, Norgren N, Giovannoni G, Fratta P, Sidle K, Fish M, Orrell R, Howard R, Talbot K, Greensmith L, Kuhle J, Turner MR, Malaspina A (2015). “Neurofilament Light Chain: A Prognostic Biomarker in Amyotrophic Lateral Sclerosis.” *Neurology*, **84**(22), 2247–2257. doi:10.1212/wnl.0000000000001642.
- Martínez-Camblor P, Pardo-Fernández JC (2018). “Smooth Time-Dependent Receiver Operating Characteristic Curve Estimators.” *Statistical Methods in Medical Research*, **27**(3), 651–674. doi:10.1177/0962280217740786.

- Pepe MS (1997). “A Regression Modelling Framework for Receiver Operating Characteristic Curves in Medical Diagnostic Testing.” *Biometrika*, **84**(3), 595–608. doi:10.1093/biomet/84.3.595.
- Pepe MS, Janes H, Longton G, Leisenring W, Newcomb P (2004). “Limitations of the Odds Ratio in Gauging the Performance of a Diagnostic, Prognostic, or Screening Marker.” *American Journal of Epidemiology*, **159**(9), 882–890. doi:10.1093/aje/kwh101.
- Pérez-Fernández S, Martínez-Cambolor P, Filzmoser P, Corral N (2018). “nsROC: An R package for Non-Standard ROC Curve Analysis.” *The R Journal*, **10**(2), 55–77. doi:10.32614/RJ-2018-043.
- R Core Team (2024). *R: A Language and Environment for Statistical Computing*. R Foundation for Statistical Computing, Vienna, Austria. URL <https://www.R-project.org/>.
- Rodríguez-Álvarez MX, Meira-Machado L, Abu-Assi E, Raposeiras-Roubín S (2016). “Non-parametric Estimation of Time-Dependent ROC Curves Conditional on a Continuous Covariate.” *Statistics in Medicine*, **35**(7), 1090–1102. doi:10.1002/sim.6769.
- Sewak A, Hothorn T (2023). “Estimating Transformations for Evaluating Diagnostic Tests with Covariate Adjustment.” *Statistical Methods in Medical Research*, **32**(7), 1403–1419. doi:10.1177/09622802231176030.
- Slate EH, Turnbull BW (2000). “Statistical Models for Longitudinal Biomarkers of Disease Onset.” *Statistics in Medicine*, **19**(4), 617–637. doi:10.1002/(sici)1097-0258(20000229)19:4<617::aid-sim360>3.0.co;2-r.
- Song X, Zhou XH (2008). “A Semiparametric Approach for the Covariate Specific ROC Curve with Survival Outcome.” *Statistica Sinica*, **18**(3), 947–965.
- Stensrud MJ, Hernán MA (2025). “Invited Commentary: Why Use Methods That Require Proportional Hazards?” *American Journal of Epidemiology*, p. kwae361. doi:10.1093/aje/kwae361.
- Taga A, Maragakis NJ (2018). “Current and Emerging ALS Biomarkers: Utility and Potential in Clinical Trials.” *Expert Review of Neurotherapeutics*, **18**(11), 871–886. doi:10.1080/14737175.2018.1530987.
- Tamasi B (2024). *tramME: Transformation Models with Mixed Effects*. doi:10.32614/CRAN.package.tramME. R package version 1.0.7.
- Tamási B (2025). “Mixed-effects Additive Transformation Models with the R Package **tramME**.” *Journal of Statistical Software*. Accepted for publication, URL <https://cran.r-project.org/web/packages/tramME/vignettes/tramME-JSS.pdf>.
- Yu D, Hwang WT (2019). “Optimal Cutoffs for Continuous Biomarkers for Survival Data under Competing Risks.” *Communications in Statistics-Simulation and Computation*, **48**(5), 1330–1345. doi:10.1080/03610918.2017.1410713.
- Zoccolella S, Beghi E, Palagano G, Fraddosio A, Guerra V, Samarelli V, Lepore V, Simone IL, Lamberti P, Serlenga L, Logroscino G, for the SLAP Registry (2008). “Analysis of

Survival and Prognostic Factors in Amyotrophic Lateral Sclerosis: A Population Based Study.” *Journal of Neurology, Neurosurgery & Psychiatry*, **79**(1), 33–37. doi:10.1136/jnnp.2007.118018.

A. Alternative ROC curve definitions

The NPB framework introduces an approach to time-dependent ROC analysis by modeling the joint distribution of the biomarker and event time conditional on covariates. This strategy allows for derivation of various ROC curve types, including incident-dynamic and incident-static, as well as associated summary indices such as the AUC and Youden Index. Unlike many existing methods, which are tailored to specific definitions of sensitivity or specificity, the NPB framework provides a way to derive all forms of time-dependent ROC curves.

A.1. Incident-dynamic

The *incident* sensitivity is the probability that a subject's biomarker value exceeds a threshold c at the exact time they experience the event

$$\text{Se}_t^{\mathbb{I}}(c | \mathbf{x}) = \text{P}(Y > c | T = t, \mathbf{X} = \mathbf{x})$$

In this definition, cases are defined as subjects experiencing the event at time t , while subjects who experienced the event before t are excluded from the calculation. This leads to the *incident-dynamic* ROC curve, which evaluates the biomarker's ability to distinguish between subjects experiencing the event at $T = t$ and those who have not yet experienced it. This measure is particularly valuable for guiding treatment decisions at multiple time points.

Under the NPB framework, where the conditional distribution of the biomarker given event time is normal, incident sensitivity has a closed-form expression

$$\begin{aligned} \text{Se}_t^{\mathbb{I}}(c | \mathbf{x}) &= \Phi \left(\frac{\rho h_T(t | \mathbf{x}) - h_Y(c | \mathbf{x})}{\sqrt{1 - \rho^2}} \right) \\ &= \Phi \left(\frac{\mathbf{x}^\top \boldsymbol{\beta}_Y + \rho (h_T(t) - \mathbf{x}^\top \boldsymbol{\beta}_T) - h_Y(c)}{\sqrt{1 - \rho^2}} \right). \end{aligned}$$

The second form assumes linear transformation models for the marginal distributions of the biomarker and event time, as introduced in Section 4. Alternative marginal models can also be incorporated as discussed in Section 7. Note that in this setup incident sensitivity involves only the evaluation of a univariate distribution function.

A.2. Incident-static

Static sensitivity is particularly useful for comparing incident cases to control subjects who are long-term survivors, i.e., those who remain event-free throughout a fixed follow-up period $(0, t^*)$ (Etzioni *et al.* 1999). It is defined as

$$\text{Sp}^{\mathbb{D}}(c | \mathbf{x}) = \text{P}(Y \leq c | T > t^*, \mathbf{X} = \mathbf{x})$$

which leads to the *incident-static* ROC curve. Under the NPB framework, the joint model for the biomarker and event time remains the same as for the dynamic specificity case described in the main text. The key difference lies in the fact that $\text{Sp}^{\mathbb{D}}$ is no longer dependent on the value of t . Instead it focuses on a fixed follow-up time t^* which is prespecified to a value which is considered a long enough time to observe the event of interest. The dependence on t is then restricted to the incident sensitivity component.

B. Additional simulation results

B.1. Simulations with different settings

This section presents additional simulations assessing the NPB framework. We use different event time distributions, sample sizes and censoring rates.

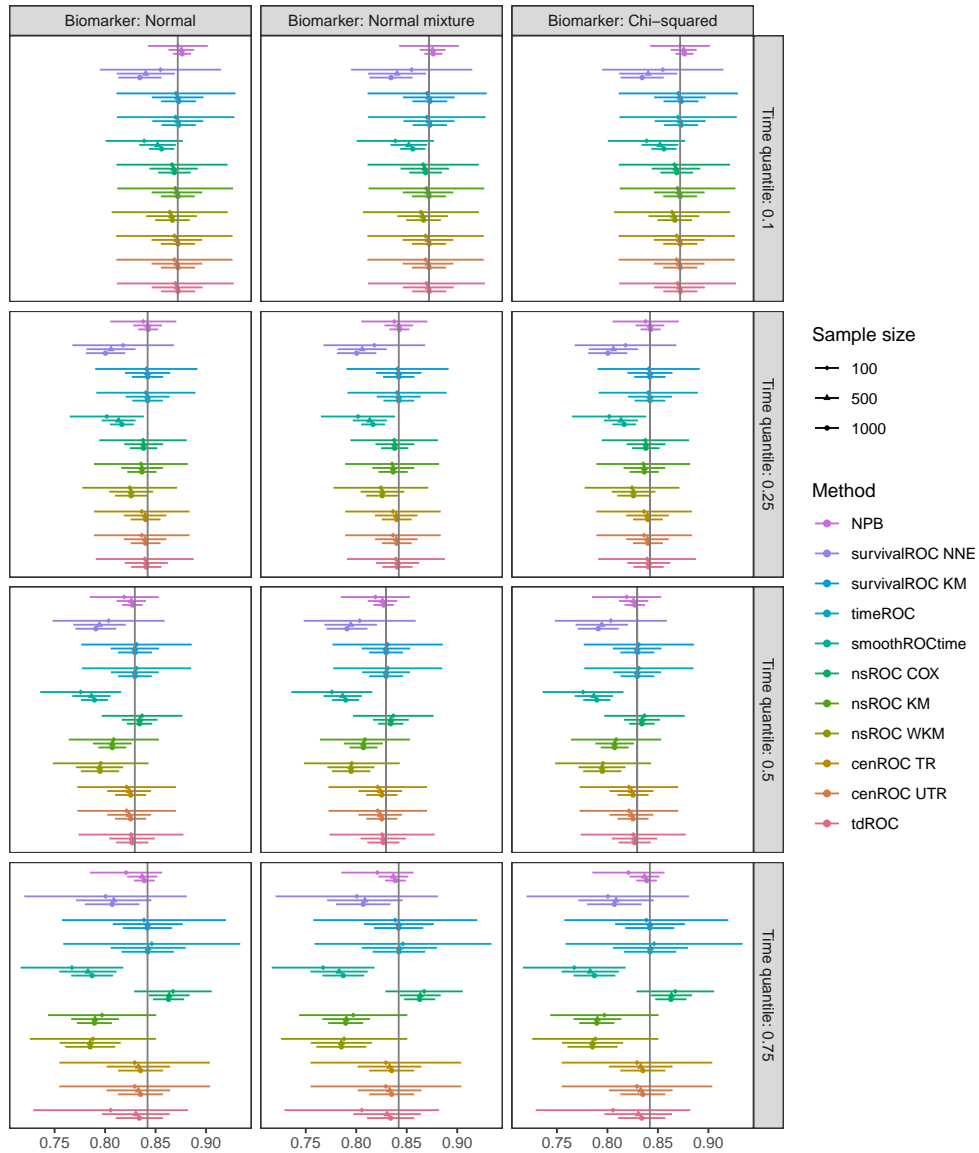


Figure 9: Mean and standard deviation of the unconditional AUC for each method with sample sizes of $N = \{100, 500, 1000\}$, Lognormal event time distribution, 50% censoring rate and a correlation of $\rho = -0.7$ between transformed biomarker and event time distributions. The evaluation is across different biomarker distributions (Normal, Normal mixture, Chi-squared) and time quantiles (0.1, 0.25, 0.5, 0.75).

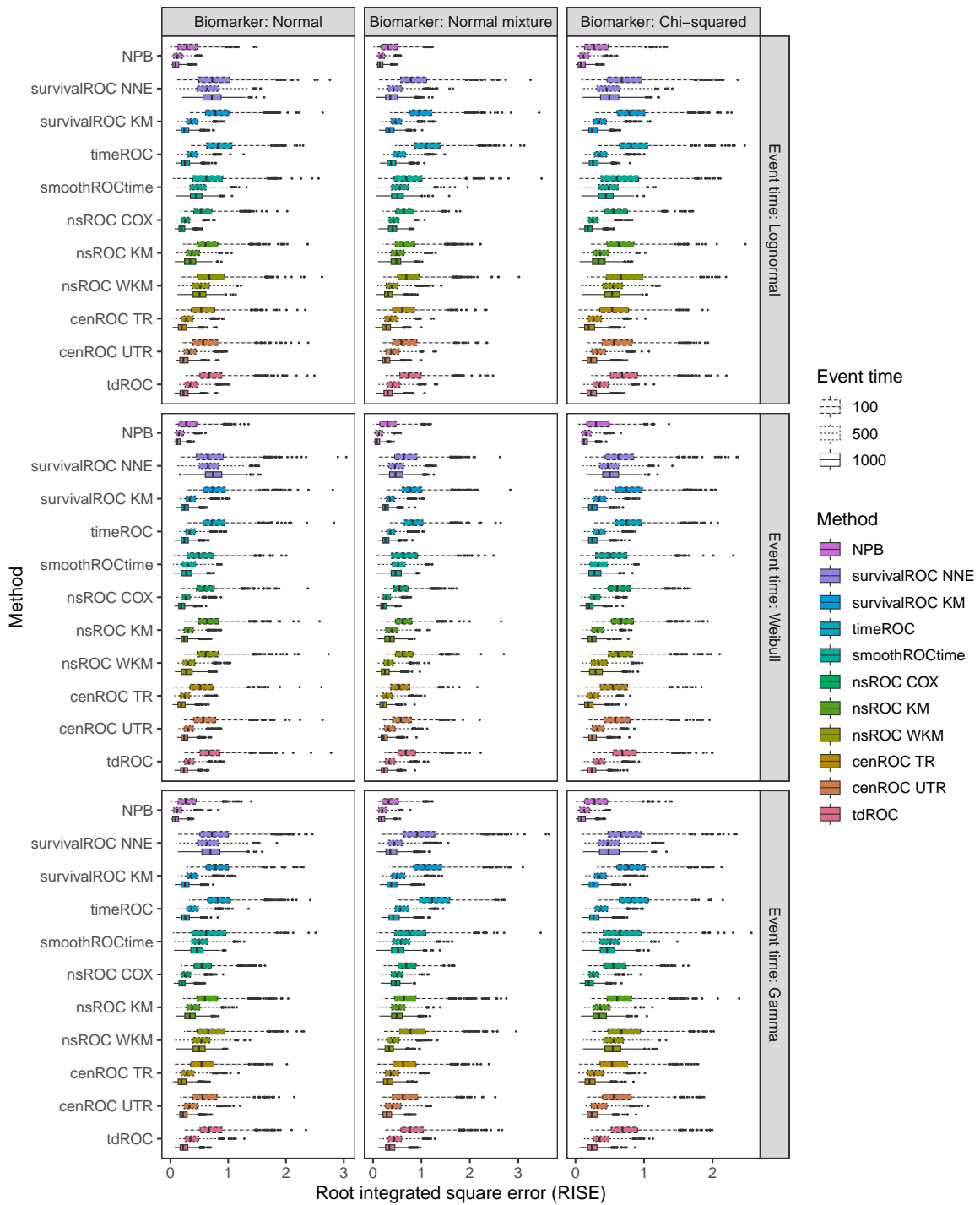


Figure 10: Distribution of root integrated squared errors (RISE) for unconditional ROC estimators at the median time quantile with sample sizes of $N \in \{100, 500, 1000\}$, event time distributions of $\{\text{Lognormal, Weibull, Gamma}\}$, 50% censoring rate and a correlation of $\rho = -0.7$ between transformed biomarker and event time distributions.

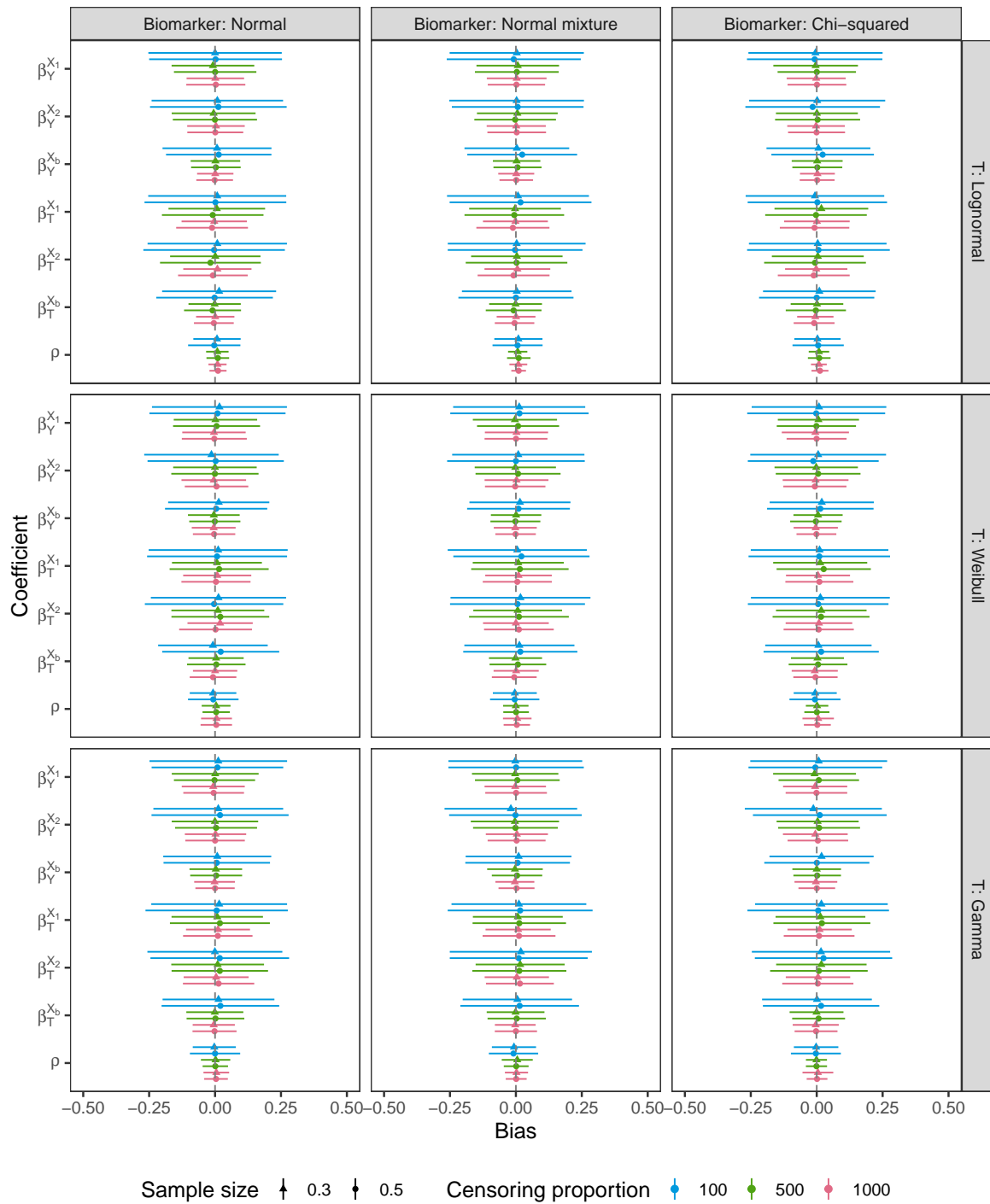


Figure 11: Mean and standard deviation of bias for coefficients for the NPB method with sample sizes of $N \in \{100, 500, 1000\}$, censoring rates of 30% and 50%, and a correlation of $\rho = -0.5$. Results are presented for varying biomarker distributions {Normal, Normal mixture, Chi-squared} and event time distributions {Lognormal, Weibull, Gamma}.

B.2. Simulations with dependence misspecification

We investigated how the NPB model performs when there is a misspecification of the dependence structure. For this, we considered an alternative DGP proposed by [Rodríguez-Álvarez *et al.* \(2016\)](#). In this setting the true relationship between the biomarker and event time deviates from the assumed copula-based dependence structure.

The covariate \mathbf{X} is generated from a normal distribution with mean 1 and variance 1, i.e., $\mathbf{X} \sim N(1, 1)$. The biomarker Y is then generated from a conditional normal distribution with mean $X = x$ and variance 1, i.e., $Y \sim N(x, 1)$. Finally, the survival time T is generated from a proportional hazards Weibull model, conditional on the biomarker and covariate. This corresponds to an accelerated failure time (AFT) model

$$\log(T) = y + 0.5x + Z,$$

where Z follows a minimum extreme value distribution.

To assess performance, we generated 1000 replications, with each dataset consisting of 500 observations with a censoring rate of 30%. We evaluated the covariate-specific cumulative-dynamic time-dependent ROC curves $\text{ROC}_t^{\text{C/D}}(x)$ 25th, 50th, and 75th percentiles of the covariate. [Figure 12](#) displays functional boxplots of the results and compares the different covariate-specific time-dependent ROC curve methods for a single time point of 1.5.

The NPB model shows low bias for low quantiles of X . However, the bias increases across higher quantiles. The proportional hazards-based semiparametric method of [Song and Zhou \(2008\)](#) outperformed other methods, since it correctly aligns with the true DGP. The nonparametric kernel-based approach was largely unbiased across quantiles but exhibited higher variability.

These results suggest that while the NPB model effectively captures correlation-driven dependencies between biomarkers and event times, it struggles when the dependence follows a direct functional form. That is, when T is assumed to be a function of Y and X . This highlights a fundamental bias-variance trade-off for method selection. Model-based approaches tend to provide low-variance, unbiased estimates when correctly specified but can introduce bias when the true DGP differs from the assumed model. In contrast, fully nonparametric methods are asymptotically unbiased but often suffer from high variability in finite samples, making estimation less stable. Additionally, nonparametric approaches have problems in incorporating multiple covariates. Ultimately, the choice of method depends on the specific application and the needs of the target audience.

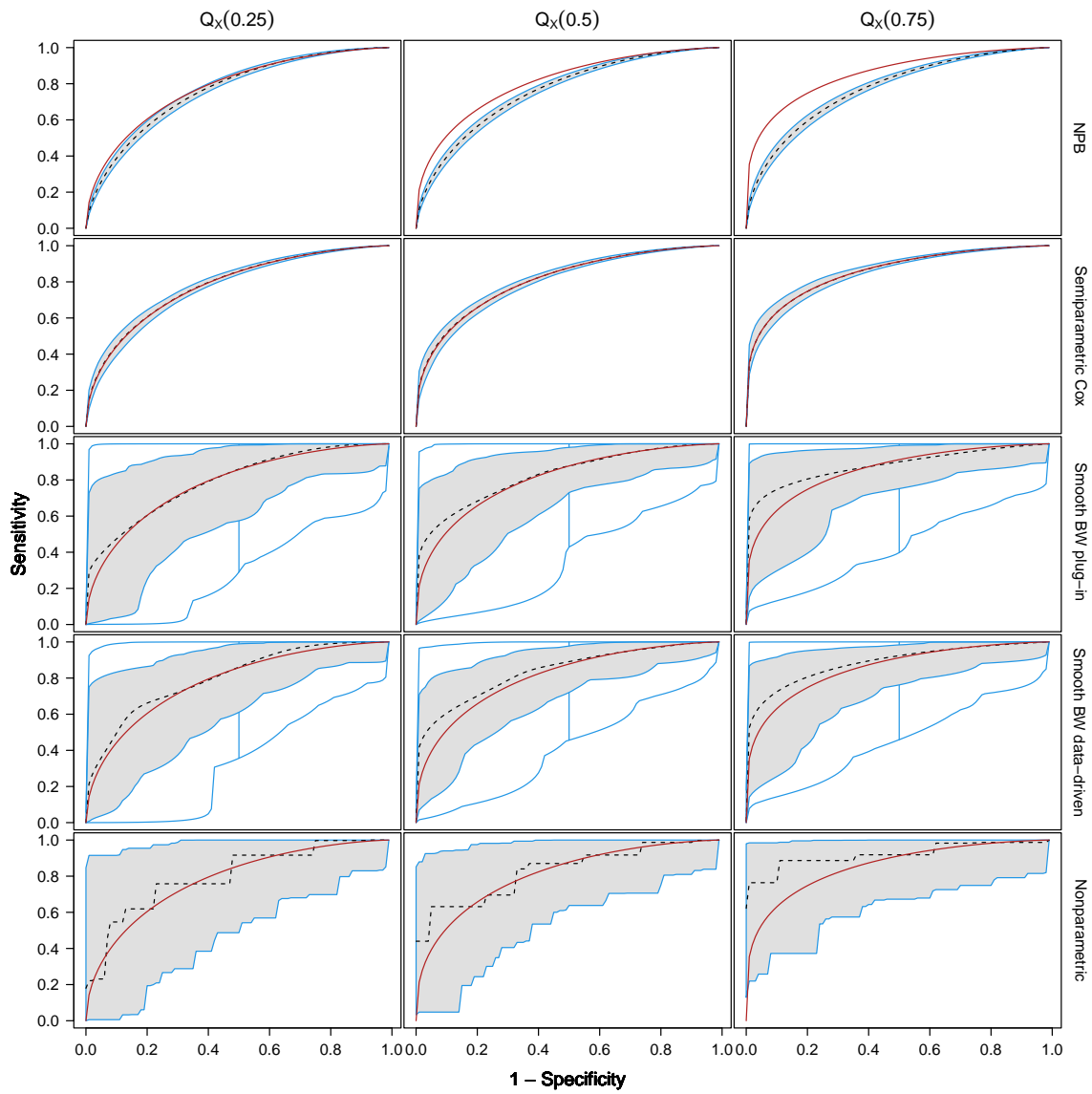


Figure 12: Functional boxplots for covariate-specific time dependent ROC curves at the median time quantile, with a sample size of $N = 500$, Weibull event time distribution, 30% censoring rate, and a correlation of $\rho = -0.5$ between transformed biomarker and event time distributions. The red line indicates the true covariate-specific ROC curve for each case.

C. Additional application results

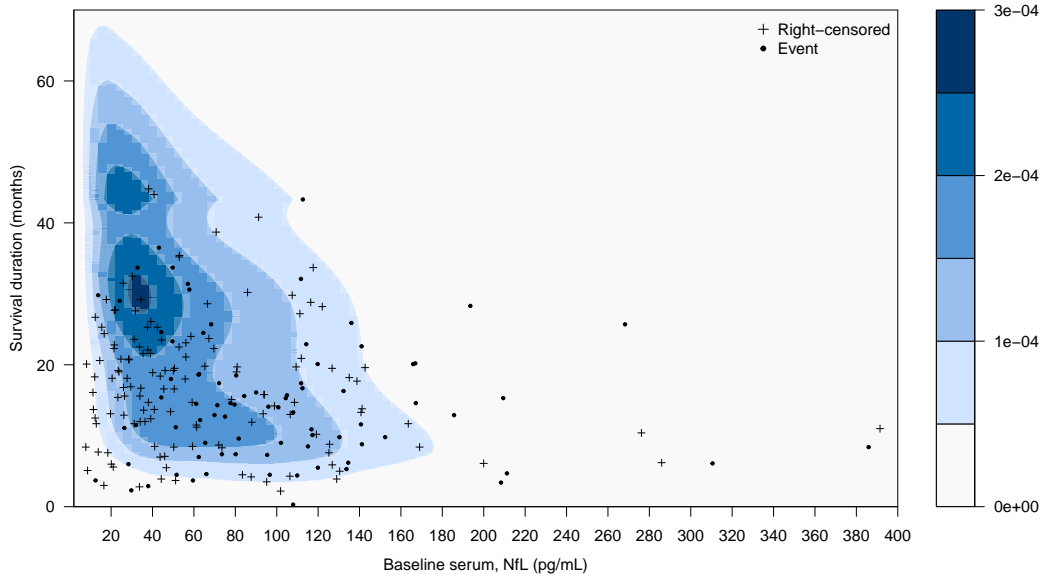


Figure 13: Estimated bivariate density of baseline serum neurofilament light (NfL) concentration (pg/mL) and survival time (in months since baseline) overlaid with observed data. Right censored subjects are indicated with “+” and subjects who reached the endpoint are marked by “.”.

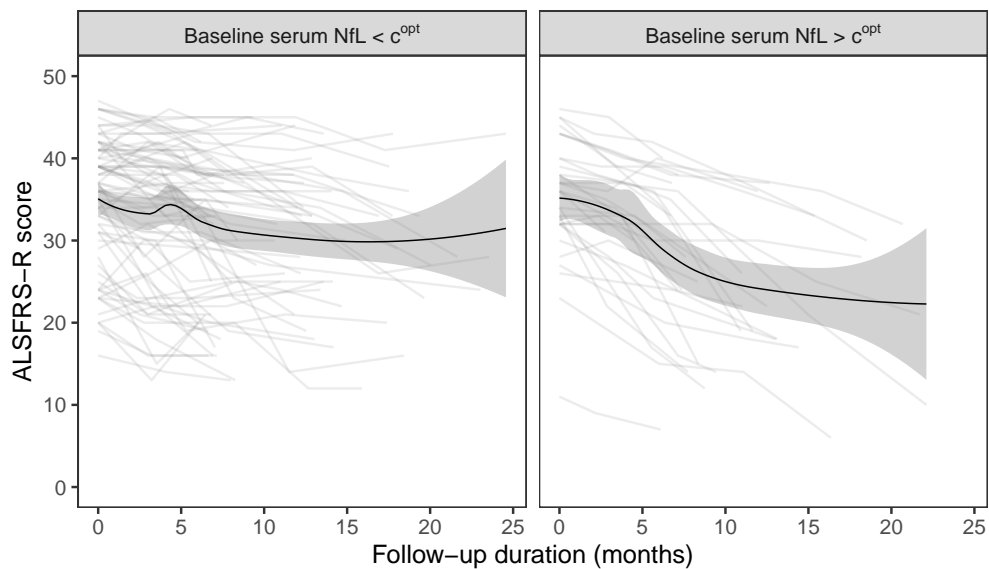


Figure 14: Spaghetti plot of ALSFRS-R scores over follow-up stratified by the optimal baseline serum neurofilament light concentration threshold for predicting 12-month survival.

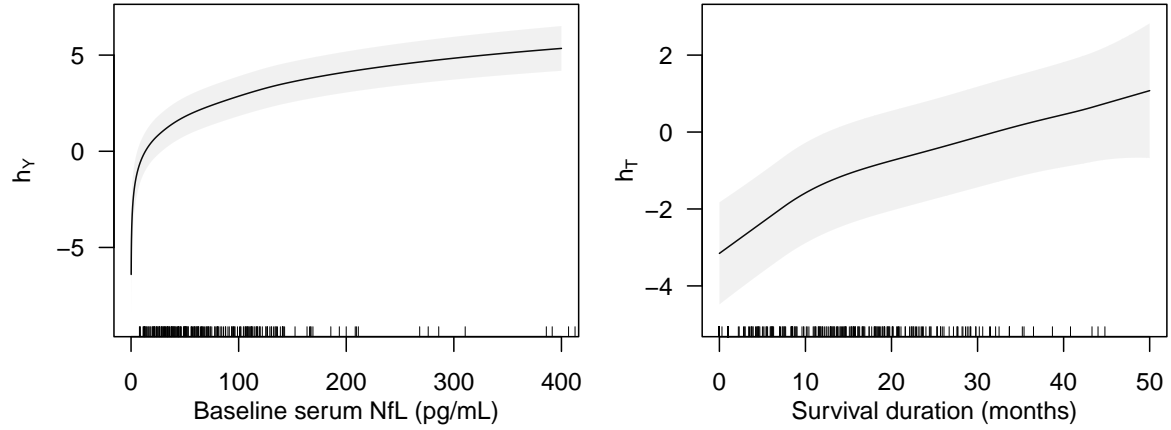


Figure 15: Estimated baseline transformation functions for baseline serum neurofilament light (NfL) concentration $h_Y(y | \hat{\vartheta}_Y)$ and survival time $h_T(t | \hat{\vartheta}_T)$.

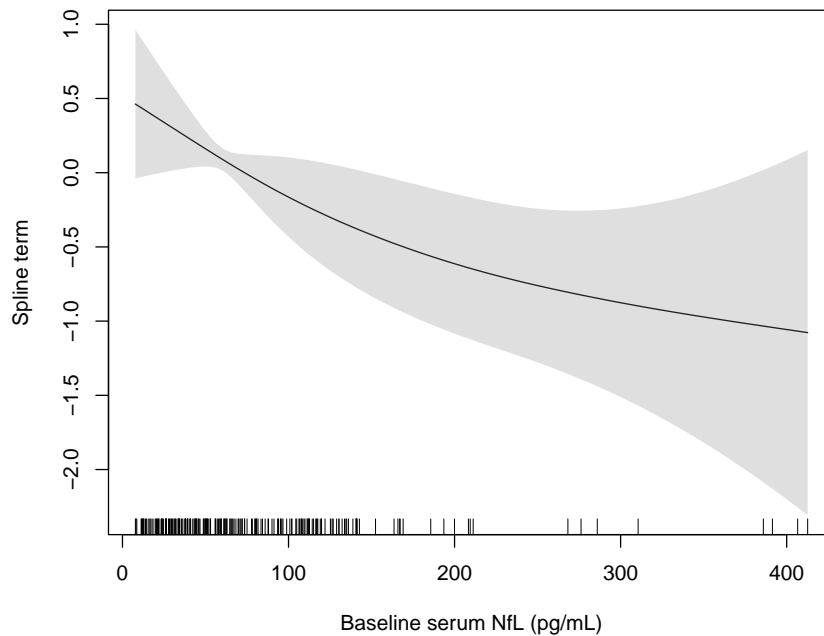


Figure 16: Spline term for NfL in a model for the conditional distribution of survival time conditioned on NfL and covariates. This is used to evaluate the assumptions of the conditional NPB model. Monotonicity of the function indicates that the Gaussian dependence structure assumption is satisfied.

Affiliation:

Ainesh Sewak
Department of Clinical Research
Universität Bern
Freiburgstrasse 3, CH-3010 Bern, Switzerland
Email: Ainesh.Sewak@unibe.ch

Vanda Inácio
School of Mathematics
University of Edinburgh
Peter Guthrie Tait Road, EH9 3FD Edinburgh, United Kingdom
Email: Vanda.Inacio@ed.ac.uk

Joanne Wu, Michael Benatar
Department of Neurology
University of Miami Miller School of Medicine
1120 NW 14th Street, Suite 1300, Miami, FL, 33136, United States
Email: MBenatar@med.miami.edu, JWuu@med.miami.edu

Torsten Hothorn
Institut für Epidemiologie, Biostatistik und Prävention
Universität Zürich
Hirschengraben 84, CH-8001 Zürich, Switzerland
Email: Torsten.Hothorn@R-project.org